Design of combination therapeutics from protein response to drugs in ovarian cancer cells

Alexandra Franz[1,2,3,*], Ciyue Shen[1,2,3,*], Fabian Coscia[4], Kenneth Munroe[5], Lea Charaoui[1,2], Anil Korkut[6], Matthias Mann[7,#], Augustin Luna[1,2,3,8,#], Chris Sander[1,2,3,#]

[1]Department of Data Science, Dana-Farber Cancer Institute, Boston, MA, 02115, USA

[2]Department of Cell Biology, Harvard Medical School, Boston, MA, 02115, USA.

[3]Broad Institute of Harvard and MIT, Cambridge, MA, 02142, USA

[4]Proteomics Program, NNF Center for Protein Research, Faculty of Health and Medical Sciences, University of Copenhagen, 2200, Copenhagen, Denmark

[5]Pharmacology Department, Charles River Laboratories, Worcester, MA 01605, USA

[6]Department of Bioinformatics and Computational Biology, UT MD Anderson Cancer Center, Houston, TX 77030, USA

[7]Department of Proteomics and Signal Transduction, Max Planck Institute of Biochemistry, 82152, Martinsried, Germany

[8]Computational Biology Branch, National Library of Medicine and Developmental Therapeutics Branch, National Cancer Institute, Bethesda, MD 20892, USA

*joint first authors

#joint corresponding authors (AL: augustin@nih.gov CS: sander.research@gmail.com)

Highlights

- 5000-protein response to 7 drugs in an ovarian cancer cell line profiled by protein mass spectrometry
- Network analysis suggested potential pathways of drug resistance inferred from response profiles
- Demonstration of a general method for profiling adaptive response to therapeutic interventions with implications for the development of anti-resistance therapy.
- Plausible anti-resistance drug combinations tested for antiproliferative effect in up to 6 ovarian cancer cell lines
- Drug combinations with additive or synergistic effects are plausible candidates for overcoming or preventing resistance to single agents
- Several combinations were synergistic (with PARPi, MEKi, and SRCi)
- We observed 0.05-0.11 micromolar response to GPX4 inhibitors as single agents in the OVCAR-4 cell line

Abstract

High-grade serous ovarian cancer (HGSOC) remains the most lethal gynecologic malignancy and novel treatment approaches are needed. Here, we used unbiased quantitative protein mass spectrometry to assess the cellular response profile to drug perturbations in ovarian cancer cells for the rational design of potential combination therapies. Analysis of the perturbation profiles revealed proteins responding across several drug perturbations (called frequently responsive below) as well as drug-specific protein responses. The frequently responsive proteins included proteins that reflected general drug resistance mechanisms such as changes in drug efflux pumps. Network analysis of drug-specific protein responses revealed known and potential novel markers of resistance, which were used to rationalize the design of anti-resistance drug pairs. We experimentally tested the anti-proliferative effects of 12 of the proposed drug combinations in 6 HGSOC cell lines. Drug combinations tested with additive or synergistic effects are plausible candidates for overcoming or preventing resistance to single agents; these include several combinations that were synergistic (with PARPi, MEKi, and SRCi). Additionally, we observed 0.05-0.11 micromolar response to GPX4 inhibitors as single agents in the OVCAR-4 cell line.

We propose several drug combinations as potential therapeutic candidates in ovarian cancer, as well as GPX4 inhibitors as single agents.

Introduction

High-grade serous ovarian cancer has an unmet clinical need

High-grade serous ovarian cancer (HGSOC) is the most common and most aggressive subtype of ovarian cancer with a high mortality rate (Matulonis et al. 2016; Siegel, Miller, and Jemal 2019). Despite surgical removal and extensive chemotherapy as first-line treatments, approximately 80% of advanced-stage tumors relapse, resulting in a 5-year survival rate of less than 30% (Colombo, Lorusso, and Scollo 2017). Only small improvements in the overall survival rate have been seen in HGSOC patients over the past decades carrying a grim prognosis (Berns and Bowtell 2012; Bowtell et al. 2015). There is thus a major unmet need for effective antitumor strategies to improve patient outcomes.

Development approaches to drug combinations in cancer

One approach to developing effective treatment regimens is the deep characterization of cancer cellular response profiles to drug perturbations. This information has not only the potential to provide predictors of therapy response but also to determine optimal drug combinations (Al-Lazikani, Banerji, and Workman 2012). For example, one combination strategy is the co-administration of drugs with similar mechanisms of action (MoAs) to enhance target coverage and inactivation of oncogenic signaling. Successful examples are pertuzumab and trastuzumab to treat $HER2^{amp}$ metastatic breast cancer (Baselga et al. 2012) and the combination of dabrafenib and trametinib to treat $BRAF^{V600E}$ melanoma (Long et al. 2016; Robert et al. 2015). Another combination strategy, which we aim for here, is to block emerging resistance pathways that are activated in response to drug treatment and plausibly represent an evasive response to perturbation. For example, compensatory activation of MEK and/or AKT has been shown to limit mTOR/PI3K inhibitor therapy in prostate and breast cancer cell lines and patient tumor samples, which could be reversed by combined inhibition of mTOR/PI3K and AKT (Carracedo

et al. 2008; O'Reilly et al. 2006). Other examples of drug pairs that work through parallel pathways and lead to enhanced anti-tumor efficacy include the combined inhibition of HER2 and PI3K in breast cancer cells (Rexer and Arteaga 2012) or co-targeting the HER family and IGF-R with afatinib and NVP-AEW541 in pancreatic cancer cells (Ioannou et al. 2013).

Available post-perturbation drug response datasets

Over the last years, there have been extensive efforts to decipher the mechanisms involved in drug response, including large-scale collections of gene expression response profiles across many cancer cell lines following drug exposure. This transcriptomics approach was pioneered by the Con-Map (Lamb et al. 2006) and extended by the NIH LINCS program (Koleti et al. 2018) and the L1000 project (Niepel et al. 2017). Considering that small molecule inhibitors usually target proteins, which are the basic functional units in biological processes, efforts have been made to collect proteomic response profiles in order to provide a more functional and proximal readout of drug action (R. F. S. Lee et al. 2017; Saei et al. 2019; Ruprecht et al. 2020; Yan et al. 2022). However, these efforts have been limited in ovarian cancer. So far, the biggest collections of drug response protein profiles in ovarian cancer cells cover 1) targeted antibody signal measurements of a total of 210 protein and phosphorylation sites by antibody-based reverse-phase protein array (RPPA) in several ovarian cancer cell lines and 2) a study focused on BET bromodomain inhibition conducted in cell lines using mass spectrometry (Zhao et al. 2020; Gonçalves et al. 2022; Kurimchak et al. 2016). Unbiased large-scale proteomic approaches are still lacking.

Identifying anti-resistance drug combinations from mass spectrometry-based proteomic profiles after drug treatment

To increase the scale of proteomic response profiles for ovarian cancer, we used unbiased deep mass spectrometry (MS)-based proteomics and comprehensively assessed the proteomic changes induced by drug action in order to identify candidate markers of resistance and provide information for drug combination strategies in ovarian cancer. We measured ovarian cancer cells' proteomic response to a number of different anti-cancer drugs (STable 2) by protein mass

spectrometry. Comparative analysis revealed specific protein responses for each of the drugs and general protein responses shared across several drugs. While we found that many generally responsive proteins in this dataset are involved in general drug resistance mechanisms (e.g., drug efflux pump), the data-driven protein network analysis of drug-specific protein responses suggested novel potential indicators of resistance response as well as known resistance indicators. Based on these observations, we propose several drug combinations for follow-up studies in ovarian cancer cells as an example of using comprehensive proteomic response profiling for the rational selection of drug combination therapeutic candidates.

Results

Computational results from proteomic response analysis to nominate drug combinations

Mass-spectrometry protein response profiling of anti-cancer compounds in ovarian cancer cells

First, we selected several anti-cancer drugs that are currently under development for the treatment of ovarian cancer patients. The selected drugs, MK-2206, Venetoclax, CHIR-99021, PD-0325901, Bisindolylmaleimide VIII (BIM VIII), and Bosutinib were selected similarly to a PARP inhibitor in our earlier study (Franz et al. 2021). Each drug targets a frequently activated oncogenic signaling pathway or biological process, such as the Akt (protein kinase B) pathway, apoptosis involving Bcl-2 (B-cell lymphoma 2), the GSK3 (glycogen synthase kinase 3) pathway, the MAPK/ERK pathway (mitogen-activated protein kinase cascade), PKC (protein kinase C) signaling, and SRC (protein tyrosine kinase) signaling. We used OVSAHO cells as a preclinical HGSOC model system as these have similar genomic and gene expression features as those measured in surgical HGSOC samples (Domcke et al. 2013; Coscia et al. 2016; Sinha et al. 2021). To explore the effects of these drugs on cellular protein levels, we perturbed OVSAHO cells with these inhibitors at their IC50 concentration (half-maximal inhibitory concentration) and measured the protein changes using MS. The IC50 for each drug was determined based on the dose-response curves derived from cell viability measured 72 hrs after drug treatment. The treatment time of 72 hrs is plausibly sufficient to capture the adaptive proteomic response of

cells upon drug treatment (Arif, Datar, and Kalsotra 2017). Cell viability was measured by cell counting using live-cell imaging (Material and Methods). Treatment with individual inhibitors resulted in a dose-dependent reduction in cell viability (Figure 1a) with IC50 values ranging from 4 µM to 12 µM (STable1). OVSAHO cells were treated at each drug's IC50 concentrations for 72 hrs in three biological replicates, and proteomic changes were profiled by MS (Figure 1b). To quantify relative protein levels across drug perturbation conditions, we applied data-independent acquisition (DIA) combined with label-free based quantification (Material and Methods). We quantified drug-perturbed protein profiles at a median depth of ~5,000 protein groups (groups are indistinguishable based on peptides identified) per perturbation condition (Figure 1c). Unsupervised multi-dimensional scaling (MDS, Euclidean distance) of biological replicates confirmed reasonable reproducibility of proteomic responses upon each drug treatment (Figure 1d).

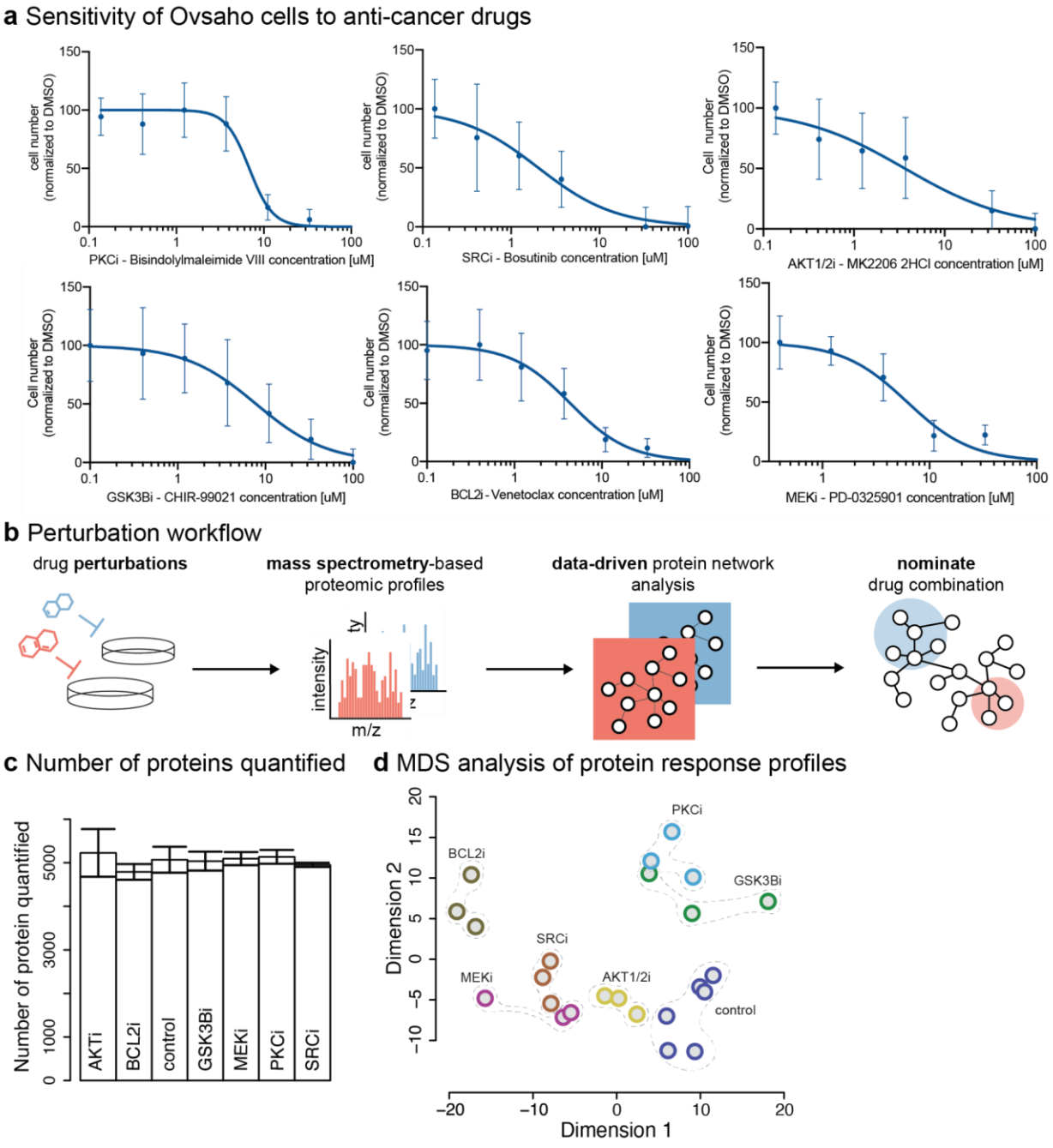

Figure 1. Acquisition of proteomic changes following molecularly targeted drug treatments in OVSAHO cells. (a) Dose-response curves of the single small-molecule inhibitors, used for the primary perturbation followed by MS protein response profiling in OVSAHO cells, including AKT inhibitor MK-2206 (AKTi), BCL2 inhibitor Venetoclax (BCL2i), GSK3β inhibitor CHIR-99021 (GSK3βi), MEK inhibitor PD-0325901 (MEKi), PKC inhibitor Bisindolylmaleimide VIII (BIM VIII, PKCi), and SRC inhibitor Bosutinib (SRCi). Data is aggregated from three biological replicates each with three technical

replicates and error bars represent standard deviations of the data. (b) Label-free mass spectrometry (MS)-based proteomics workflow used to measure protein changes in response to drug treatment at IC50. Data-driven network analysis was later applied to the acquired MS data to identify potential resistance mechanisms for the nomination of drug combination candidates. (c) Number of proteins quantified upon each drug treatment of OVSAHO cells after 72h at inhibitor IC50 concentration. Error bars: standard deviation of three biological replicates for each condition. (d) Multidimensional scaling (MDS, Euclidean distance) 2D projection of protein levels measured after treatment. Colors indicate different drug perturbation conditions with weak dotted lines around each group of biological replicates to indicate the closeness of the replicates.

Comparison of strongly responsive proteins across drug perturbation conditions

We examined the measured global proteome response for each of the six drugs and identified a total of 5858 proteins of which 4480 (76%) proteins were experimentally detected in all perturbation conditions (SFigure 1). We assessed which proteins and cellular processes were most strongly affected by the drug treatment. We defined strongly responsive proteins as proteins with an expression level change upon drug treatment compared to the control treatment of at least 0.5 or -0.5 (log2 ratio of perturbed/control) with a nominal p-value < 0.05 and BH-based FDR < 0.2 (Materials and Methods). Using these parameters, we found that most proteins (>80%) did not respond strongly across treatment conditions (Figure 2a). The different drug treatments resulted in different proportions of strongly responsive proteins, which indicates different extent and scope of downstream signaling. For example, while AKTi induced strong expression level changes in a relatively small number of proteins (8% of the measured proteins), inhibition of SRC affected as much as 18%. Indeed, SRC activity is known to have key roles in affecting multiple pathways (Mayer and Krop 2010). Across the six different perturbations, the expression levels of a total of 2714 proteins changed significantly in at least one drug condition (‘strong response’) of which only 127 proteins changed strongly in at least 4 perturbation conditions (‘frequently responsive’) (Figure 2b; STable2). Frequently affected proteins generally had expression level changes in the same direction across all drug perturbations (Figure 2c), indicating a potential general stress response. The strongly responsive proteins for each drug are used below as a guide for choosing candidates for anti-resistance drug combinations.

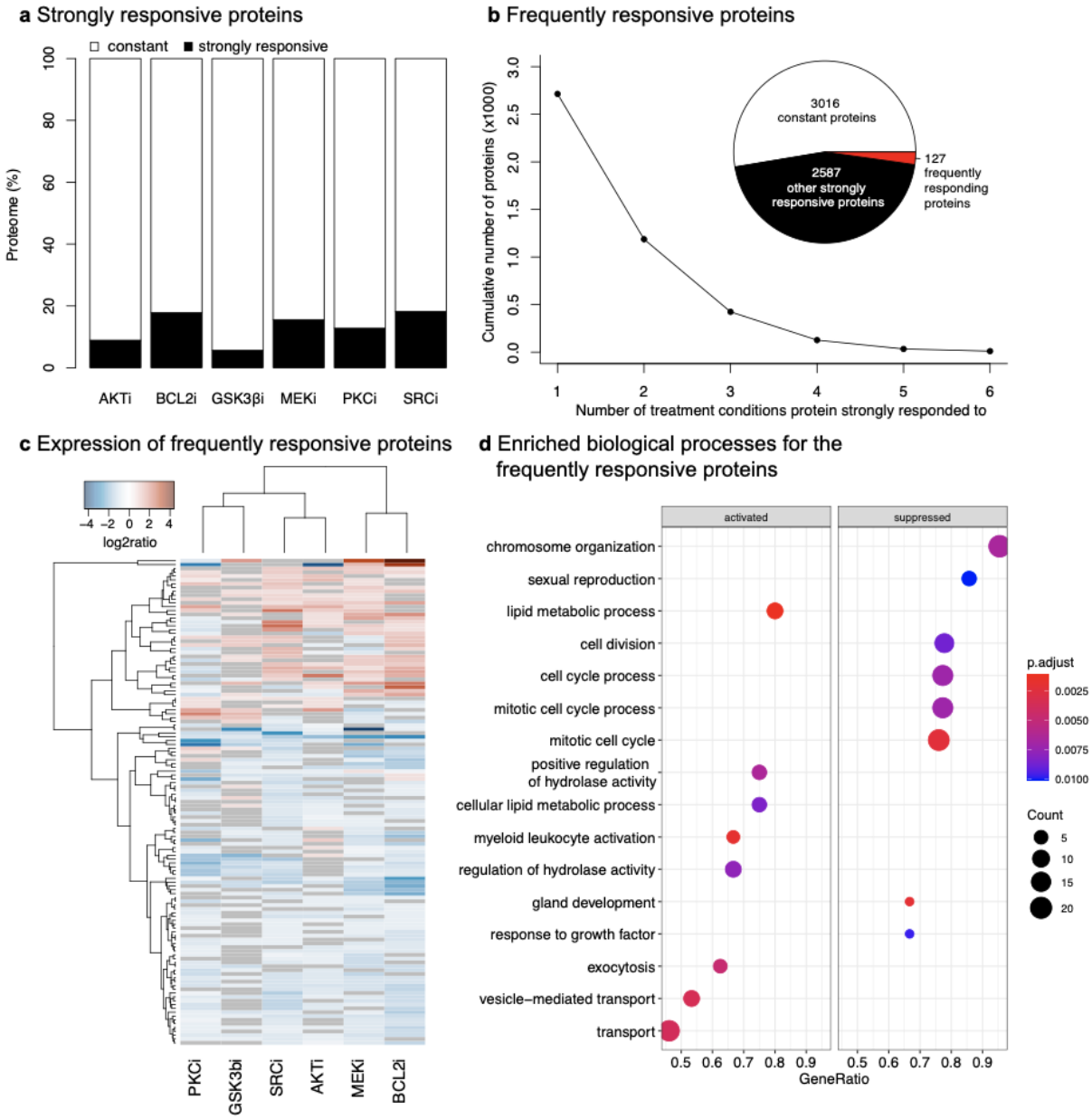

Figure 2. Identification of frequently responsive proteins and processes induced by pharmacological inhibitors. (a) Proportion of proteins per treatment condition that changed compared to the control treatment. Strongly responsive proteins are defined as proteins whose absolute log2 expression change is at least 0.5 (p-value < 0.05 and BH-based FDR < 0.2 in t-test). Constant proteins are the remaining proteins; protein expression values are averaged over three biological replicates. (b) Cumulative numbers of proteins that strongly respond to a certain number of perturbation conditions. Proteins

that strongly respond in 4 or more treatment conditions are defined as frequently responsive proteins (red). The set of 2587 drug-specific proteins (black in the pie chart) is the union of the strongly responsive proteins for the six drugs (black rectangles in (a)). (c) Protein expression change of identified frequently responsive proteins; "frequently" refers to both positively and negatively responding proteins in at least 4 conditions (red in (b)). Most proteins respond with consistent trends (e.g., increasing expression) across several or all perturbation conditions, consistent with the notion of being part of a general stress response. (d) Gene set enrichment analysis (GSEA) identified both activated (increased protein expression) and suppressed (decreased protein expression) biological processes. Suppressed processes likely reflect the cytotoxic effects of drugs while activated processes might suggest a general resistance mechanism.

Identification of general response markers to pharmacological inhibition

Several well-known resistance mechanisms have been observed to develop in cancer cells against different pharmacological compounds that are structurally and functionally unrelated (Zelcer et al. 2001). Therefore, we next assessed the functional properties of the 127 frequently responsive proteins. Using gene set enrichment analysis (GSEA) (Subramanian et al. 2005), we found that levels of proteins involved in cell survival and proliferation were significantly decreased, including in biological processes such as chromosome organization (GO:0051276, p-value = 6.63E-03), and cell cycle processes (GO:0022402, p-value = 7.18E-03) (Figure 2d). In contrast, biological processes, such as lipid metabolic processes (GO:0006629, p-value = 1.19E-03), vesicle-mediated transport (GO:0016192, p-value = 3.54E-03), and positive regulation of hydrolase activity (GO:0051345, p-value = 6.43E-03) included proteins with significantly increased expression as a consequence of drug perturbation. Consistent with previous research on the response of cancer cells under stressed environments (Munir et al. 2019; Q. Wu et al. 2021), these up-regulated processes are likely general adaptive responses of ovarian cancer cells to pharmacological inhibition.

Identification of drug-specific response markers and nomination of drug combinations

We next analyzed strongly responsive proteins for each individual drug treatment condition to gain further insight into drug-specific cellular response. We applied three independent and

complementary computational approaches to nominate drug-responsive proteins and pathways. The approaches include the NetBox algorithm for module detection (Cerami et al. 2010; Liu et al. 2020), gene set enrichment analysis (GSEA) (Subramanian et al. 2005), and interpretation of individual protein expression changes by inspection of functional annotations. The NetBox algorithm combines prior knowledge of protein interaction networks with a clustering algorithm to identify functional protein modules. We used the NetBox algorithm to identify likely functional protein modules and used annotations of individual protein functions of module members to functionally label each module (Material and Methods). We applied GSEA to independently identify affected biological processes by each drug inhibition. In addition, we examined individual responsive proteins that are reported to have a role in known cancer signaling. For each of the small-molecule drugs, the functional annotation of the identified protein modules with decreased activities generally agreed with the known inhibitory roles of the drugs (Figure 3a, Supplementary notes, SFigure 2). The identified modules and their protein members are of particular interest as they are likely indicative of potential adaptation or resistance mechanisms to the small-molecule inhibitors.

247 **Figure 3a**

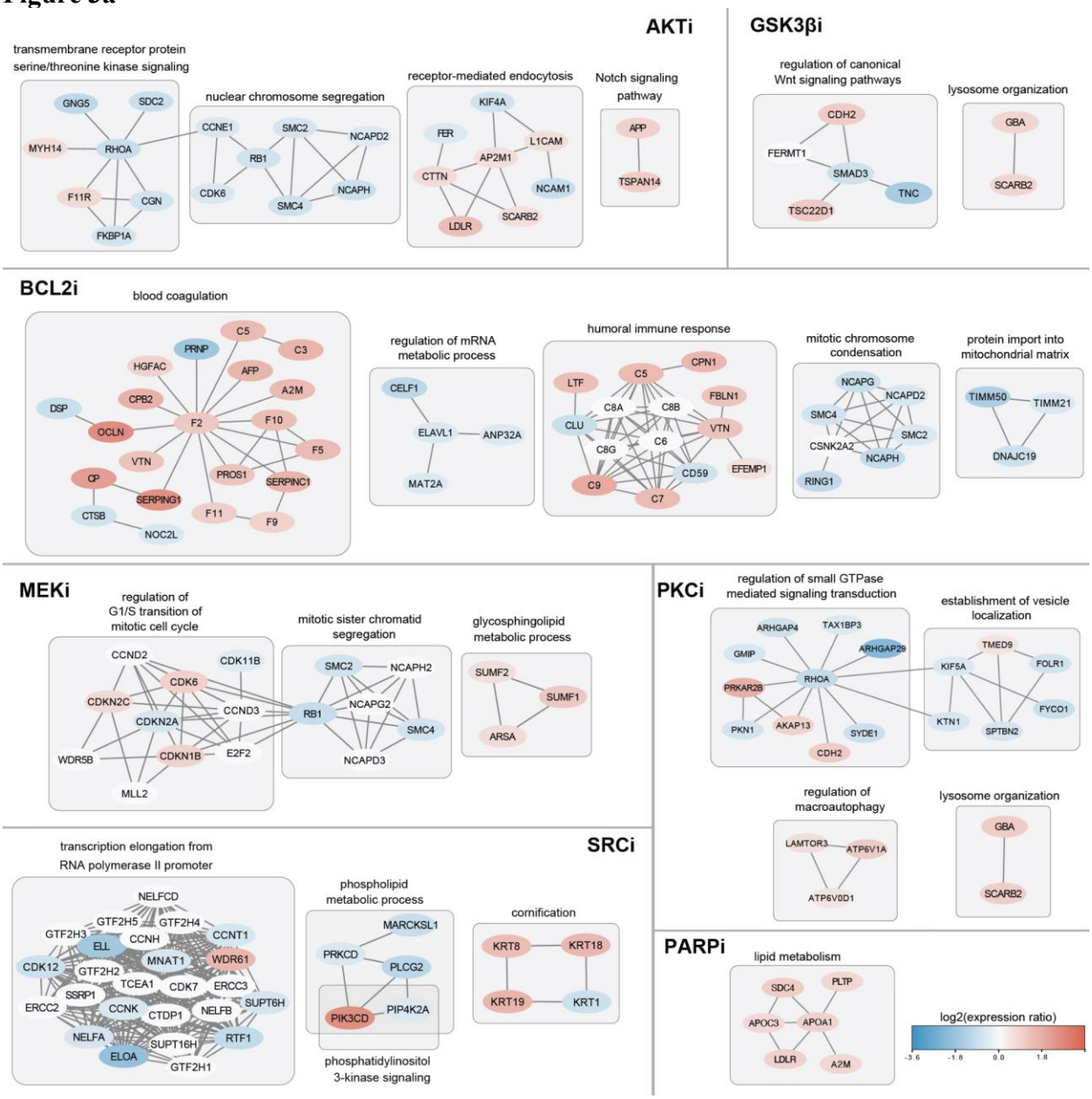

248
249

250

Figure 3b

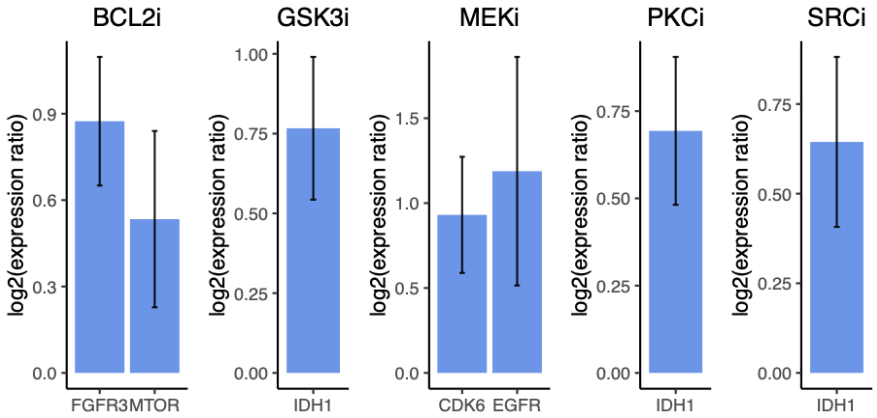

Figure 3. Drug-specific protein response networks identified using NetBox.

(**a**) Drug-specific protein responses were grouped into functional modules using the NetBox algorithm and the modules were characterized by functional labels based on enrichment analysis (Material and Methods). Subsets of protein modules for each drug perturbation were chosen based on their relevance to the known functions of the inhibitors and their implications for potential resistance mechanisms. Nodes are proteins colored by protein expression change, log2(expression ratio perturbed/unperturbed). Edges are undirected protein interactions from the background network used by the NetBox algorithm (Reactome FI Network or INDRA network). (**b**) Individual protein expression change ratios that are justification for the nominated drug combinations.

We identified potential resistance mechanisms as protein modules and biological processes that are pro-proliferative and increased in activity, as indicated by an increase in average protein expression; or anti-proliferative and decreased in activity. Whether a given protein or a biological process is pro-proliferative or anti-proliferative is defined as an individual functional score (1: pro-proliferative or -1: anti-proliferative) for the protein or the average functional score of the proteins in the process (Materials and Methods). To nominate potentially therapeutic drug combinations, we suggest targeting proteins involved in the presumed resistance mechanisms together with the original small-molecule target, with the intent to block the restoration of proliferation. The candidate drugs were chosen as specific inhibitors of the selected pathways (Table 1). We then ranked the drug combination candidates based on their clinical stages, prioritizing drugs approved by the U.S. Food and Drug Administration (FDA) (e.g., rucaparib, an

approved treatment versus AG14361, an experimental compound). To further filter the candidates, we also reviewed previous literature on how widely these candidates have been used in preclinical studies, as well as additional supporting information on resistance mechanisms and potential drug pairs in combination therapies (see Supplementary notes).

Tested drug (A)	Combination partner (B)	Target of B	Mechanism of B	Clinical stage of B	Analysis evidence
AKTi (MK-2206)	AL101 (BMS-906024)	NOTCH signaling	γ-secretase inhibitor	FDA fast track designation for adenoid cystic carcinoma	Netbox analysis
BCL2i (Venetoclax)	Infigratinib	FGFR signaling	FGFR1-3 inhibitor	FDA-approved for cholangiocarcinoma	Individual protein
BCL2i (Venetoclax)	Everolimus	MTOR signaling	mTORC1 inhibitor	FDA-approved for breast cancer, renal cell carcinoma, etc.	Individual protein
GSK3βi (CHIR-99021)	Ivosidenib	IDH1	Isocitrate dehydrogenase-1 inhibitor	FDA-approved for acute myeloid leukemia and cholangiocarcinoma	Individual protein
MEKi (PD-0325901)	Erlotinib	EGFR signaling	EGFR tyrosine kinase inhibitor	FDA-approved for pancreatic & non-small cell lung cancer (NSCLC)	Individual protein
MEKi (PD-0325901)	Palbociclib	CDK4/6	CDK4/6 inhibitor	FDA-approved for breast cancer	Individual protein
PKCi (BIM VIII)	Ivosidenib	IDH1	Isocitrate dehydrogenase-1 inhibitor	FDA-approved for acute myeloid leukemia & cholangiocarcinoma	Individual protein
PKCi (BIM VIII)	TVB-2640	FASN	Fatty acid synthetase inhibitor	FDA fast track designation for nonalcoholic steatohepatitis (NASH)	GSEA analysis
SRCi (Bosutinib)	Idelalisib	PI3K signaling	PI3K delta isoform inhibitor	FDA-approved for chronic lymphocytic leukemia and lymphoma	Netbox analysis
SRCi (Bosutinib)	Ivosidenib	IDH1	Isocitrate dehydrogenase-1 inhibitor	FDA-approved for acute myeloid leukemia and cholangiocarcinoma	Individual protein
SRCi (Bosutinib)	Auranofin	Redox enzymes	Inhibition of redox enzymes	FDA-approved for rheumatoid arthritis, clinical trials in cancer	Individual protein & NetBox
PARPi (Rucaparib)	TVB-2640	FASN	Lipid synthesis	FDA fast track designation for nonalcoholic steatohepatitis (NASH)	Netbox analysis
PARPi (Rucaparib)	GC7	DHSP	eIF5A hypusination inhibitor	Pre-clinical	Netbox analysis
PARPi (Rucaparib)	Apcin	APC–CDC20	Anaphase (Cdc20 inhibitor)	Pre-clinical	Netbox analysis
PARPi (Rucaparib)	Simvastatin	HMGCR	Lipids (PLTP)	FDA-approved for lowering lipids	Netbox analysis
PARPi (Rucaparib)	RSL3	GPX4	Ferroptosis activator	Pre-clinical	Netbox analysis
PARPi (Rucaparib)	GPX4-IN-3	GPX4	Ferroptosis activator	Pre-clinical	Netbox analysis

Table 1. Proposed combination drug candidates based on the analysis of the proteomic response profiles. These combinations were tested experimentally. Potential resistance mechanisms were identified based on the analysis of proteomic profiling after drug treatment using three complementary approaches, (i.e., NetBox analysis, GSEA analysis, and individual protein expression analysis). Small molecule inhibitors were selected to target the corresponding pathways indicative of resistance as combination partners of the originally profiled drugs. Drugs are prioritized if they are more relevant in clinical settings, i.e. FDA-approved or in late-stage clinical trials.

Potential drug combination candidates with PARPi

Identifying drug pairs for combination intervention is meant to address the problem of lack of sensitivity to PARPi in some ovarian tumors in a clinical setting; an active area of research (Dréan, Lord, and Ashworth 2016). Our computational results indicate that an inferred module of interest with increased protein expression after perturbation with the PARPi olaparib in OVSAHO cells contains a set of proteins involved in lipid metabolism and lipoprotein processes and reported to pairwise interact (Figure 3a): A2M (alpha 2 macroglobulin, interacts with APO lipoproteins), SDC4 (syndecan4, a plasma membrane proteoglycan), PLTP (a phospholipid transfer protein, involved in the transfer of excess surface lipids from triglyceride-rich

lipoproteins to HDL and involved in the uptake of cholesterol from peripheral cells and tissues), LDLR (a member of the low-density lipoprotein receptors family), APOC3 (reported to promote the assembly and secretion of triglyceride-rich VLDL particles) and ApoA1 (a protein component of high-density lipoprotein particles).

As the abundance of each of these five functionally connected proteins increased after PARPi perturbation, we searched for drugs that affect cellular processes involving lipids or lipoproteins by targeting these proteins directly or indirectly. After inspection of pathway knowledge bases and background knowledge of mechanisms of resistance to PARP inhibition, we chose the following drugs to be combined with PARPi. (1) TVB, a fatty acid synthase (FASN) inhibitor, which reduces fatty acid turnover. (2) RSL3 and GPX4-IN-3, both inhibitors of GPX4. GPX4 is a selenoprotein that reduces lipid hydroperoxides and prevents ferroptosis in conditions of oxidative stress (ROS) with enhanced lipid peroxidation, to the advantage of surviving cancer cells (Yang et al. 2014). Ferroptosis is a form of regulated cell death characterized by the accumulation of lipid peroxides; so, inhibiting GPX4 promotes ferroptosis, reducing cell count. (3) Simvastatin, an inhibitor of HMG-CoA reductase (HMGR), is an enzyme in the mevalonate pathway and the rate-limiting enzyme in cholesterol biosynthesis; the reason for inclusion is that statins are reported to have many pleiotropic effects downstream of the mevalonate pathway and to have anti-invasive and anti-inflammatory effects supporting a repurposed anti-cancer use (Matusewicz et al. 2015) (Zaky et al. 2023). In addition, as motivated in our previous report (Franz et al. 2021) we also added the drugs (4) GC7, inhibitor of deoxyhypusine synthase, and (5) apcin, inhibitor of activity of the anaphase-promoting complex APC/C to be combined with PARP inhibition (Table 1). An additional proposed combination involves rucaparib with novobiocin, an inhibitor of polymerase theta, motivated independently (not as a result of our proteomics screen) due to interest in the work of d'Andrea et al. (Iorio et al. 2016; Zhou et al. 2021), who reported that BRCA-deficient tumor cells with acquired resistance to PARPi are sensitive to novobiocin in vitro and in vivo.

Potential drug combination candidates with AKTi

We observed that upon AKT inhibition, a NetBox-identified protein module enriched for the Notch signaling pathway (GO:0007219, adj. p-value = 2.37E-02) has increased expression levels with an average log2 expression ratio (after/before perturbation) of 0.99 over two genes, APP and TSPAN14. Activation of Notch signaling is found in different types of cancer and inhibition of Notch signaling has been shown as a potential therapeutic approach (Katoh and Katoh 2020). Thus, the upregulation of proteins in Notch signaling pathways might be an adaptive mechanism for ovarian cancer cells to resist AKT inhibition. Therefore, we propose to use AL101 (BMS-906024), a γ-secretase inhibitor, which blocks Notch activity by preventing cleavage of the Notch receptors at the cell surface (Olsauskas-Kuprys, Zlobin, and Osipo 2013) in combination with the AKT inhibitor.

Potential drug combination candidates with BCL2i

We identified two pro-proliferative genes whose protein expression increased upon BCL2 inhibition, FGFR3 (log2ratio = 0.87, p-value = 2.00E-03) and MTOR (log2ratio = 0.53, p-value = 3.49E-02), which have well-known roles in cancer signaling, i.e., FGFR signaling, and mTOR signaling (Figure 3b). With additional evidence from previous literature reporting enhanced anti-tumor effects of dual inhibition (inhibition of Bcl-2 and FGFR in endometrial cancer; and of Bcl-2 and mTOR in renal cell carcinoma) (Packer et al. 2019; Nayman et al. 2019), we hypothesize that both signaling pathways may be able to implement resistance to BCL2 inhibition in OVCA and may contain reasonable combination targets with BCL2i. We chose Infigratinib**,** a selective FGFR1-3 inhibitor to target FGFR signaling (FDA-approved for treatment of cholangiocarcinoma with an FGFR2 fusion), and Everolimus which inhibits the formation of the mTOR complex, for testing in combination with BCL2i. Everolimus has been the subject of Phase I and II clinical trials testing certain drug combinations in ovarian cancer (NCT01281514, NCT00886691).

Potential drug combination candidates with GSK3βi

We found that the protein expression of isocitrate dehydrogenase 1 (IDH1) increased upon GSK3β inhibition (log2ratio = 0.767, p-value = 1.40E-03) (Figure 3b). It has been previously reported that pharmacological inhibition or knockdown of IDH1 decreased proliferation by inducing senescence in multiple HGSOC cell lines (Dahl et al. 2019). Therefore, we believe IDH1 can be a resistance marker for GSK3β inhibition. We select Ivosidenib, an FDA-approved inhibitor for IDH1, as the combination partner for GSK3βi.

We also found that the NetBox-identified protein module enriched for lysosome organization (GO:0007040, adj. p-value = 1.18E-03) is activated. This response has been previously reported by Albrecht et. al (Albrecht et al. 2020) who observed that macropinocytosis, triggered by GSK3-inhibition, induced catabolic activity of lysosomes. We believe increased lysosome activity might be a resistance mechanism to GSK3β inhibition. The lysosome is linked to many hallmarks of cancer and a wide range of agents have been shown to affect multiple aspects of lysosome activities in clinical trials (Davidson and Vander Heiden 2017). We believe our analysis does not provide sufficient evidence to support our choice of drug(s) inhibiting a particular lysosomal target. Therefore, experimental validation of co-targeting GSK3β and lysosome activities is beyond the scope of this study.

Potential drug combination candidates with MEKi

The protein expression of EGFR (log2ratio = 1.19, p-value = 1.01E-02) increased upon MEK inhibition (Figure 3b). Previous literature demonstrated that combined inhibition of MEK and EGFR prevents the emergence of resistance in EGFR-mutant lung cancer. We, therefore, selected the most widely used EGFR inhibitor Erlotinib as the combination partner with our MEKi. We also observed that the expression of cyclin-dependent kinase 6 (CDK6) increased in response to MEK inhibition (log2ratio = 0.931, p-value = 4.55E-03), which positively affects the cell cycle. Since CDK6 is a potential resistance marker of MEKi, as well as a single therapeutic

target for ovarian cancer patients (Dall'Acqua et al. 2021), we selected palbociclib as the specific inhibitor of CDK4/6 to use in combination with MEKi.

We found an increase in the expression of proteins enriched for the glycosphingolipid metabolic process (GO:0006687, adj. p-value = 3.51E-07) using NetBox. Interestingly, metabolic rewiring in response to MEK inhibition has been previously described as a possible mechanism of resistance in melanoma cells (Ruocco et al. 2019; Nguyen et al. 2020), and targeting of lipid metabolism has been previously reported in ovarian cancer cells (Chen et al. 2019). Although targeting highly expressed metabolic enzymes in the glycosphingolipid metabolic process might provide a potential strategy to overcome MEKi resistance in ovarian cancer, this hypothesis has yet to be tested due to the lack of specific inhibitors of the pathway.

Potential drug combination candidates with PKCi

The results of GSEA suggested that proteins involved in lipid metabolic process (GO:0006629, p-value = 1.13E-03) have increased expression upon PKC inhibition. Lipid metabolic processes have been identified as part of general stress response and as potential targets for combination therapy (Chen et al. 2019; Snaebjornsson, Janaki-Raman, and Schulze 2020). Therefore, we selected TVB-2640, a fatty acid synthase inhibitor to target this resistance mechanism. Similar to our observations with GSK3β inhibition, IDH1 (log2ratio = 0.694, p-value = 1.81E-03), as well as proteins involved in the process of lysosome organization (GO:0007040, adj. p-value = 1.24E-05) have increased expression upon PKCi (Figure 3b). We propose Ivosidenib with PKCi as a potential combination candidate.

Potential drug combination candidates with SRCi

We found that one responsive protein module identified by NetBox is enriched for proteins involved in the phospholipid metabolic process (GO:0006644, adj. p-value = 4.86E-04). An interesting observation is that two proteins, PI3K delta isoform (PIK3CD) and phosphatidylinositol-5-phosphate 4-kinase type-2 alpha (PIP4K2A) in this module are also involved in the PI3K signaling pathway, which is critical for cell survival and frequently altered

in ovarian cancer. Although SRC inhibition has been previously reported to suppress the PI3K pathway (Beadnell et al. 2018), our observation suggested that the protein expression of the PI3K delta isoform significantly increased upon SRC inhibition (log2ratio = 2.48, p-value = 1.77E-03). Therefore, we propose to use Idelalisib, a specific PI3K delta isoform inhibitor, in combination with SRCi. The combination of SRC and PI3K (by saracatinib and GDC-0941, respectively) has been shown to be effective in renal cancer in several pre-clinical models, including PDX models (Roelants et al. 2018). We also observed an increase in protein expression of IDH1 upon SRC inhibition (log2ratio = 0.644, p-value = 2.76E-03) and therefore propose Ivosidenib and SRCi as a combination candidate (Figure 3b). In addition, we observed that the protein expressions of peroxiredoxins II (log2ratio = 0.754, p-value = 2.87E-03) and V (log2ratio = 0.821, p-value = 8.95E-04) (PRDX) are significantly increased. PRDXs are antioxidant enzymes that play key roles in regulating peroxide levels within cells controlling various physiological functions (Perkins et al. 2015). Several studies have implicated an increase of reactive oxygen species (ROS) in carcinogenesis due to a loss of proper redox control (Nicolussi et al. 2017). Most notably, in ovarian cancer cells, PRDX expression was found to be associated with platinum drug resistance (X.-Y. Wang, Wang, and Li 2013) since increased levels of antioxidants inhibit apoptosis (Kalinina et al. 2012). Our NetBox analysis with strongly responsive proteins identified a module labeled detoxification of ROS (data not shown). Our observations together with the reported results of others suggest that PRDXs are promising resistance markers to be targeted together with SRCi. Therefore, to target peroxiredoxins and the antioxidation process, we select auranofin, which inhibits the redox enzymes. Although not specific, auranofin is the closest to clinical use in cancer compared to all other inhibitors of antioxidation (Bajor et al. 2020).

Experimental results on nominated drug combinations

Choice of cell lines for experimental validation

We experimentally tested the cellular response to drug combination candidates (Table 2, SFigure 3) proposed by our computational analysis of the protein perturbation response data (Table 1) that includes combinations based on our earlier work (Franz et al. 2021).

Full Names	Short Names	Mechanism	IGROV-1	OVCAR-4	OVCAR-5	OVCAR-8	OVSAHO	TOV-21G
Rucaparib+TVB-2640	Ruc+TVB	PARP + FASN	1.133	0.426	1.472	0.172	1.629	1.752
Rucaparib+Apcin	Ruc+Apcin	PARP + Anaphase-Promoting Complex (APC)	1.010	0.955	1.653	0.517	1.820	1.426
Rucaparib+GC7	Ruc+GC7	PARP + DNA Synthase	0.467	1.263	1.522	0.307	1.636	1.587
Rucaparib+Novobiocin	Ruc+Novo	PARP + DNA Pol	1.488	1.612	1.559	1.264	1.083	1.839
Rucaparib+RSL3	Ruc+RSL3	PARP + GPX4	1.215	2.516	1.644	1.326	1.752	1.720
Rucaparib+GPX4-IN-3	Ruc+GPX	PARP + GPX4	1.202	1.995	1.463	1.234	1.455	1.191
Rucaparib+Simvastatin	Ruc+Sim	PARP + Statin	1.039	1.663	1.359	0.896	1.334	1.185
PD-0325901+Palbociclib	PD+Pal	MEK + CDK4/6	0.816	0.408	0.367	0.732	0.341	NA
Venetoclax+Infigratinib	Ven+Inf	BCL2 + FGFR3	3.515	1.496	1.312	1.214	1.014	1.520
Venetoclax+Everolimus	Ven+Eve	BCL2 + MTOR	1.690	1.082	1.487	0.797	0.975	1.033
Bosutinib+Idelalisib	Bos+Ide	SRC + PI3K	0.855	1.273	1.110	0.788	4.124	0.564
Bosutinib+Auranofin	Bos+Aur	SRC + PRDX	1.081	0.822	1.188	0.929	1.056	0.948

Table 2 Drug combinations experimentally tested for effect on proliferation. The most interesting drug combinations were experimentally tested across several ovarian cell lines and the inferred combination indices (CI) were calculated by the Chou-Talalay method. For drug combinations with 3 technical replicates, cell response was averaged across the replicates to perform the CI computation. CI < 1.00 indicates synergy (red) and CI > 1.00 the opposite. IGROV-1 etc (columns) are cell lines. NA: not available for technical reasons.

We first tested each of the drug combinations in the OVSAHO cell line. For selected candidate combinations, including several with synergistic effects, we further tested the general validity of the anti-proliferative effects in another 5 HGSOC cell lines covering diverse genetic backgrounds (IGROV-1, OVCAR-4, OVCAR-5, OVCAR-8, and TOV-21G) (Table 2). These cell lines reflect a range of genomic and proteomic features of HGSOC patient tumors (Table 3). With respect to rucaparib, the cell lines used here cover a range of sensitivities. They have IC-50s for the PARPi rucaparib in the range of 13 to 206 uM as reported in the Genomics of Drug Sensitivity in Cancer (GDSC2, v8.5) dataset (Iorio et al. 2016) with OVCAR-4 and OVCAR-5 being the least sensitive to PARP inhibition (the OVSAHO cell line is not in GDSC) (Table 3). Together with OVASHO, these cell lines reflect well-defined preclinical models of HGSOC (Domcke et al. 2013; Coscia et al. 2016; Sinha et al. 2021). For each of the drug combinations, we measured cell viability after 72 hours.

Cell Line	GDSC Rucaparib IC50 (uM)	TC Similarity to Tumors (Higher Better)	Domcke Similarity to Tumors Rank (47 Total; Smaller Better)	Replication Time	# Mutations (cBioPortal)	# CNAs (cBioPortal)	KRAS	BRCA1	BRCA2	ATM	ATR	PTEN	PIK3CA	RB1	TP53
IGROV-1	13.45	0.46	43	20-30 h	273	360		✔	✔	✔		✔	✔	✔	✔
OVCAR-4	116.08	0.99	5	34-41 h	38	2355			✔	✔	✔	✔			✔
OVCAR-5	208.32	0.46	NA	27-50 h	NA	NA	✔								
OVCAR-8	36.98	0.7	26	24-32 h	42	1349	✔			✔					✔
TOV-21G	35.88	0.13	47	27-36 h	154	147	✔					✔	✔		
OVSAHO	NA	NA	2	36-72 h	32	1118			✔					✔	✔

Table 3 OVCA HGSOC cell line measures of similarity to patient samples and drug response to rucaparib. Cell line similarity to TCGA HGSOC patient samples as characterized by Domcke et al. and TumorComparer (TC) (Sinha et al. 2021; Domcke et al. 2013). Additionally, a select set of genes including ones commonly altered in HGSOC (i.e., BRCA1, BRCA2, RB1) (Cancer Genome Atlas Research Network 2011). Rucaparib IC50 (µM, half-maximal inhibitory concentration) single drug screening of the cell lines as reported in Genomics of Drug Sensitivity in Cancer (GDSC) (Iorio et al. 2016). Mutations are protein-coding mutations as measured in particular cell line studies; similarly, CNAs are copy number alterations. KRAS etc. are proteins, altered (green check) or not (blank) by mutation or CNA.

Several combinations with PARPi are synergistic in ovarian cancer cells

For clinical therapeutic applications, both additive and synergistic combination drug effects are of interest. On the one hand, synergy implies an initial effect that is stronger than additive, deemed to be beneficial since side effects decrease with lower drug concentration. On the other hand, if resistance develops to one of the drugs, synergy is also lost, which is disadvantageous. Additionally, it is possible to see the benefit of combination therapy due to variable response in the population even without synergy or additivity (Palmer and Sorger 2017).

For the purpose of careful consideration for future pre-clinical investigation, we do report synergy values for all drug combinations for which there is sufficiently clear data. To quantify drug synergy (Combination Index, CI) we used the Chou-Talalay method (Chou 2010). We observe that some combinations of PARP inhibition via rucaparib with compounds targeting several other targets have synergistic effects (CI: < 1) in 2 of the 6 HGSOC cell lines: with (i) a fatty acid synthase inhibitor (TVB-2640), (ii) an APC inhibitor (Apcin), and (iii) an eIF5A-2 inhibitor (GC7). For PARP+APC and PARP+FASN inhibition, we observe synergistic effects in both OVCAR-4 and OVCAR-8. The synergistic effect of PARP+FASN inhibition is most

striking in OVCAR-8: the antiproliferative effect of the combination is nearly 6 times stronger than that of the single drugs. There was weak synergy (approximate additivity) using the rucaparib and apcin combination (CI: 0.955) in OVCAR-4. Across the drug combinations tested with rucaparib, OVCAR-8 had the most synergistic effects across the drug combinations tested (8 out of 12, Table 2). Interestingly, the use of the FDA-approved rucaparib PARP inhibitor did not produce the same additive or synergistic effects as combinations (inhibitors of FASN, APC, DNA synthesis, proteasome) with an alternative experimental PARP inhibitor (AG-14361), presumably due to differences in drug action on PARP activity.

Effects of combinations targeting GPX4 in ovarian cancer cells

A separate category of combinations tested experimentally involved the protein GPX4. GPX4 dependencies can arise in some therapy-resistant cancers (Hangauer et al. 2017; X. Wu et al. 2022). Both RSL3 and GPX4-IN-3 are preclinical compounds. Neither of these combinations resulted in synergistic combinations as defined by the CI value. We did however observe that GPX4 inhibitors have a remarkably strong single agent effect in the cell lines tested, in the OVCAR-4 cell line at an IC50 of 0.11 micromolar for GPX4-IN3 and 0.05 for RSL3 (Figure 4, STable 3). It has been reported that an R245W mutation in TP53 may produce a protective effect to RSL3 in triple-negative breast cancer (TNBC) (Dibra et al. 2024). However, OVCAR-4 has a different mutation in TP53 (L130V) and that does not appear to have a protective effect against GPX4 inhibition given the strong response we observe. Separately, there have been previous reports of synergistic combination effects with the alternative PARP inhibitor, olaparib, with RSL3 in the HEY HGSOC cell line; HEY is a G12D KRAS-mutated line (Hong et al. 2021). The authors of the previous study suggest that this combination works due to an adaptive response whereby GPX4 is induced in response to olaparib treatment. However, the sensitivity to single-agent GPX4 inhibition may be more general and have other explanations (Lei et al. 2024); detailed exploration of this is beyond the scope of the current study.

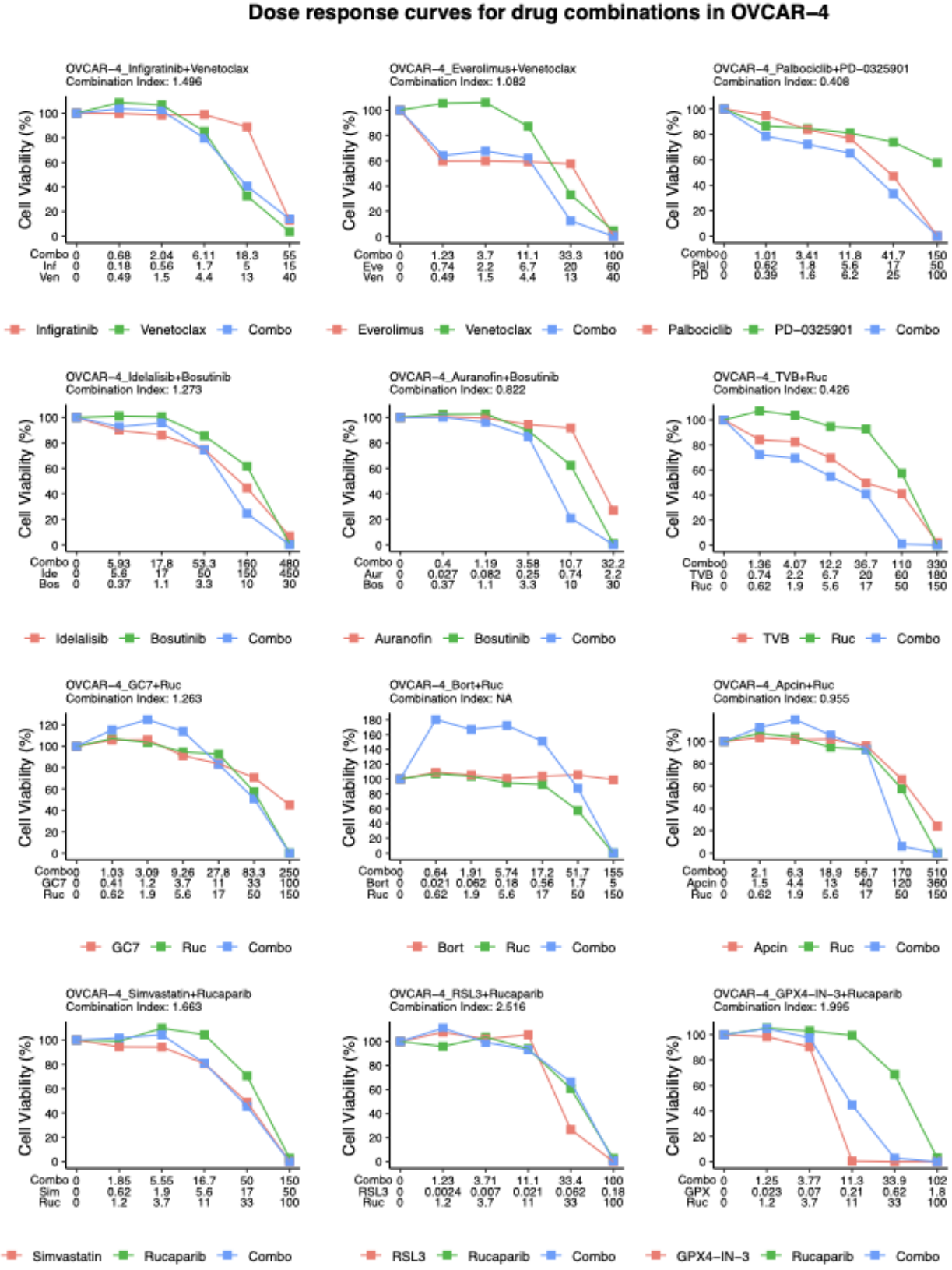

Figure 4. Inhibition of proliferation by various drug combinations in a representative ovarian cancer cell line (OVCAR-4). The combinations were chosen based on pathway analysis of protein response (Fig. 3). TVB-2640 ('TVB', FASNi), rucaparib ('Ruc', PARPi), bortezomib ('Bort', proteasome inhibitor), Apcin (APCi), GC7 (DNA synthase inhibitor), novobiocin ('Novo', DNA polymerase inhibitor), infigratinib ('Inf', FGFR3i), venetoclax ('Ven', BCL2i), everolimus ('Eve', MTORi), Palbociclib ('Pal', CDK4/6i), PD-0325901 ('PD', MEKi), idelalisib ('Ide', PI3Ki), bosutinib ('Bos', SRCi), auranofin ('Aur', PRDXi), simvastatin ('Sim', statin), GPX4-IN-3 ('GPX', GPX4i), RSL3 (GPX4i), DM4 (tubulin inhibitor). Each drug was applied to OVCAR-4 cells with a serial dilution factor of 3 or 4 to establish a dose-response curve for the single drug. Each drug combination was applied at the same concentrations as the single drugs. The combination index for each drug pair is calculated using the Chou-Talalay method.

Several combinations with MEKi and SRCi are synergistic in ovarian cancer cells

The drug combination with synergy across most cell lines (based on CI) was the PD-0325901+Palbociclib drug combination targeting MEK and CDK4/6, respectively. This drug combination has been studied pre-clinically in colorectal cancer (C. L. Lee et al. 2023) and is the subject of an ongoing clinical trial for solid tumors (NCT02022982).

Several drug combinations including those targeting NOTCH + AKT, MEK + EGFR, PKC + FASN, and those targeting IDH1 were only tested in the OVSAHO cell line due to resource limitations (STable 1). Two of the drug combinations with bosutinib (SRCi) - adding Idelalisib (PI3Ki) or Auranofin (PRDXi) - had synergistic effects in OVCAR-8 and TOV-21G (Table 2).

Discussion

Summary of the current study

There is great interest in rational approaches to the identification of drug combinations that can overcome initially present or acquired drug resistance in cancer. Adaptation to the stress of treatment can occur within a matter of days as cellular processes respond to support survival

(Marine, Dawson, and Dawson 2020) (Bell et al. 2019). We conducted a comprehensive evaluation of protein level changes in high-grade serous ovarian cancer (HGSOC) using mass spectrometry (MS) to obtain insight into markers and mechanisms of resistance. In our single agent experiments using 7 drugs targeting key cancer processes (e.g., WNT, RAS/RAF/MEK, PI3K/AKT, apoptosis, etc.), we identified responses in specific cellular processes using NetBox (see Methods) analysis that groups proteomic responses into functional modules. Suitable member proteins of a module were flagged as targets of a second agent in combination with the initial drug to prevent or overcome resistance. These hypotheses were followed up experimentally on a subset of several cell lines that reasonably represent the diversity of HGSOC patient samples, as assessed by the similarity of genomic and expression profiles of the cell lines to those of HGSOC surgical samples, as reported in TCGA datasets (Table 3) (Domcke et al. 2013; Sinha et al. 2021).

Relationships of tested cell line genetics and combination responses

This workflow revealed several effective drug combinations. Building on our previous work on PARP inhibitors, we see that PARPi+FASNi has a strong anti-proliferative effect versus single agent PARPi in OVCAR8 cells, which aligns with a growing interest in the importance of lipid metabolism in ovarian cancer and possible therapeutic implications (Yoon and Lee 2022; Chaudhry, Thomas, and Simmons 2022; Ji et al. 2020). Related to lipid requirements of cell proliferation, we did explore the combination of PARPi (rucaparib) with statins (i.e., simvastatin), which target HMG-CoA reductase, a key enzyme in the mevalonate pathway. With this combination, we also see a synergistic effect in the OVCAR8 cell line. The unique genomic profile of the OVCAR8 may contribute to these observations. OVCAR8 has an AA-changing mutation (V613L; variant of unknown significance, VUS) in the ATM gene that is related to homologous recombination (HR) and has no other HR-related mutations (Table 3). Unique to OVCAR8 is a KRAS P121H in a loop near the G base of GTP, which may affect GDP/GTP exchange. We do see some overlap in drug-drug synergy patterns between the OVCAR8 and the OVCAR4 cell lines; we see synergy involving PARPi+APCi in both OVCAR8 and OVCAR4. Both cell lines have been reported by several groups as HR proficient and both have an ATM mutation (N230T in OVCAR4, a VUS) (Wilson et al. 2018; Kondrashova et al. 2018; Siddiqui et

al. 2021; Lu et al. 2022). The results using combinations with PARPi build on our previous discussion on the therapeutic benefit of PARP inhibition regardless of HR status (Franz et al. 2021; González-Martín et al. 2019).

Ongoing interest in GPX4

Regarding HR deficiency, recent work has shown that BRCA1-deficiency may be important to the response of cancer cells co-treated with a GPX4 and PARP combination, where GPX4 inhibition can induce ferroptosis (Lei et al. 2024). Of the cell lines we selected, only IGROV-1 is BRCA1-deficient therefore it is difficult to draw conclusive direct comparisons. Of the ovarian cell lines tested in this study, IGROV1, OVCAR4, and OVSAHO are BRCA2-deficient that could affect response. In related work, in HT1080 fibrosarcoma BRCA2-knockout cells, Lei et al. do not observe a difference in RSL3 response (Lei et al. 2024). Across the cell lines tested, we see no synergy as measured by the combination index with a GPX4i and PARPi combination (Table 2). That said, our treated cell lines were highly responsive to both of the tested GPX4 inhibitors as single agents (RSL3 and GPX4-IN-3; IC50 0.5 uM and 0.11 uM), suggesting further preclinical work. One issue hampering the further development of RSL3 for clinical application is its reported low aqueous solubility (Gaschler et al. 2018; L. Wang, Chen, and Yan 2022). There is continuing research to develop novel GPX4 inhibitor chemistry, as well as means of targeted delivery to overcome existing limitations (Eaton et al. 2020; W. Li et al. 2022; Gao et al. 2019). Separately, other groups are exploring other novel combinations utilizing GPX4 inhibition. NRF2/GPX4 (RSL3) combinations in ovarian cancer and head and neck cancer (N. Li et al. 2024; Shin et al. 2018) and taxol in GPX4 inhibit the proliferation of cell lines (Feng et al. 2023). The rationale for the NRF2/GPX4 combination is that NRF2 is a regulator of anti-ferroptic genes, including genes that prevent the accumulation of free iron (Dodson, Castro-Portuguez, and Zhang 2019). This work with GPX4 is of particular interest, as there have been observations of resistance to platinum-based treatments and GPX4 levels in ovarian patients (X. Wu et al. 2022). So both single-agent inhibition of GPX4 and combinations may be particularly promising for pre-clinical studies in ovarian cancer.

Further possible pre-clinical work

For the successful combinations and single agent result we describe here, further study in more advanced preclinical models (e.g., organoids, patient-derived xenografts, (PDXs)) is warranted, but outside of the scope of the current work. If conducted, such studies could provide an initial assessment of toxicity for the proposed drug combinations, as well as some understanding of the effectiveness of the treatment in the presence of immune cells. To our knowledge, none of the proposed drug combinations have been subject to clinical trials specific to ovarian cancer. In future work, we expect to extend our experimentation to PDXs. Another consideration for future study is that in our experiments, cells were simultaneously treated with a given drug combination. Staggered (or sequential) treatment preclinical studies are less common though it is not uncommon for patients to receive a sequence of anti-cancer treatments. Several preclinical studies demonstrate the efficacy of this staggered approach and work through their mechanistic rationale (Settleman, Neto, and Bernards 2021; M. J. Lee et al. 2012). Specific to PARPi treatments, there is some evidence for the utility of PARPi in combination with other treatments (BETi and WEEi) under a given sequential regimen (Fang et al. 2019; Peng et al. 2024). Computationally reliable predictive techniques that optimize sequential multi-drug treatments remain elusive; it is an open research question.

Possibilities for future developments at larger scales

In previous work, we developed a perturbation biology framework (CellBox) (Yuan et al. 2021) for the derivation of computational models predictive of the cellular response to perturbations of any one of the many proteins observed in perturbation-response experiments, or even of combinations of proteins. Such models would be potentially more powerful and replace the module-plus-target-identification analysis used here, but their parameterization requires a much larger number of systematic perturbation experiments: probably hundreds or thousands of targeted perturbations, many more than the seven used here. This scale-up remains an open challenge and an opportunity, provided by the scale of thousands of protein levels quantitatively measurable by mass spectrometry. The work presented here provides guidance to the design of ongoing efforts that make use of comprehensive protein and phosphoprotein changes resulting

from the perturbation of key cancer processes (Kupcik et al. 2019)(J. Li et al. 2022; Franciosa et al. 2023)(J. Li et al. 2022).

Materials and Methods

Drug perturbation experiments for proteomic profiling

OVSAHO cells were obtained from JCRB (Japanese Collection of Research Bioresources Cell Bank) cell bank (NIBIOHN, Cell No. JCRB 1046) and grown in MCDB105/199 medium supplemented with 10% FBS (Fisher, #10438026) and 1% Penicillin-Streptomycin. All cells were free of Mycoplasma and their identity was verified by whole-exome sequencing at the sequencing platform of the Broad Institute of MIT and Harvard. The following drugs used in the experiments were all commercially available: AKT inhibitor MK-2206 2HCl (Selleckchem, #S1078), BCL2 inhibitor Venetoclax (ABT-199, Selleckchem, #S8048), GSK3β inhibitor CHIR-99021 (Selleckchem, #S1263), MEK inhibitor PD-0325901 (Selleckchem, #S1036), PKC inhibitor Bisindolylmaleimide VIII (Caymanchem, #13333), and SRC inhibitor Bosutinib (SKI-606, Selleckchem, #S1014). To determine the IC50 for each of the drugs, cells were treated with DMSO control or varying concentrations (from 0.01 μM to 100 μM) of each drug 24 hours after seeding. The Incucyte NucLight Rapid Red (NRR) Reagent (Essen Bioscience, #4717, 1:4000) was added to the medium to label the nuclei of live cells. Cell viability was determined as the number of live cells 72 hr after drug treatment, counted using the live imaging of Incucyte, normalized to those of the DMSO control. Cell viability data from three biological replicates each consisting of three technical replicates were merged and fitted using a non-linear log(inhibitor) versus normalized response with a variable slope for dose-response curves using GraphPad Prism. IC50 was determined as the drug concentration that gives 50% of the maximal inhibitory response on cell viability for each drug. To harvest cells for mass spectrometry proteomic profiling, cells were treated with DMSO control or the IC50 concentration 24 hr after seeding in 10 cm dishes for each drug treatment. Cells were harvested 72 hours after drug treatment by gently scraping off from the plate into PBS and transferred into deep 2 mL 96 well plates. Cells were stored at -80°C and sent for mass spectrometry measurements.

Liquid chromatography-mass spectrometry (LC-MS) measurements and MS data analysis

Harvested cells were digested and the proteomic measurements were taken as previously described (Franz et al. 2021), section 'Liquid chromatograph-mass spectrometry (LC-MS) measurements' of Methods. The raw data obtained from mass spectrometry measurements was processed as previously described (Franz et al. 2021), section 'MS data analysis' of Methods. The protein expression matrix with rows as identified proteins and columns as samples was obtained after data processing.

Proteomics data analysis

The protein expression matrix contained protein measurements from three biological replicates of each drug treatment and two sets of three biological replicates of DMSO control (due to two batches of samples). Data analysis was performed using customized scripts in R (Version 3.6). Counting the number of measured proteins, multidimensional scaling (MDS) on Euclidean distance of protein measurements, and pairwise Pearson correlation of individual samples were performed on the raw protein expression matrix. To identify differentially expressed proteins of each perturbation condition from negative controls, an unpaired t-test was used to compare protein expressions from the drug-treated samples with samples treated with DMSO. log2(expression ratio) ('log2ratio') and corrected p-values for an FDR < 0.2 by the Benjamini-Hochberg (BH) method were obtained for each drug perturbation. Strongly responsive proteins were defined as those whose log2ratio > 0.5 or < -0.5 with corrected p-value < 0.05. The protein measurements from the biological replicates were then pooled to obtain average protein expression values for each perturbation condition. The averaged protein expression across replicates was then used for unsupervised hierarchical clustering, pairwise correlation of perturbation conditions, and all the following analyses.

Protein module detection and enrichment analysis

NetBox was used to perform the detection of responsive protein modules (Cerami et al. 2010; Liu et al. 2020). For each of the drug-treatment conditions, the input gene list contains strongly responsive proteins upon the drug treatment (absolute value of log2ratio > 0.5) whose p-value of the t-test of differential expression is smaller than 0.01. To ensure the most compact and confident module findings, the adjusted p-value of the connected linker node was set to 0.005

with all the other parameters of NetBox kept at default. Two protein-protein interaction networks were used independently as the background network of NetBox analysis: 1) Reactome Functional Interaction (FI) Network (version 2020 from Reactome.org) (Gillespie et al. 2022) with predicted interactions filtered out, 2) Interactions collected by Integrated Network and Dynamical Reasoning Assembler (INDRA) with at least a belief score of 0.95 (Gyori et al. 2017), which typically indicate the interaction is supported by multiple independent reading systems or pathway databases. Enrichment analysis was performed on the identified modules using the clusterProfiler Bioconductor package (Yu et al. 2012) using gene annotations from the Gene Ontology with default parameters. Gene Set Enrichment Analysis (GSEA) (Subramanian et al. 2005), was performed on the responsive proteins using clusterProfiler with default parameters. The input gene lists for each drug treatment are consistent with those for NetBox analysis, and the ranking of the genes is based on the log2ratio of the corresponding proteins in decreasing order.

Determination of functional score

The list of cancer census genes was obtained from the Catalogue of Somatic Mutations In Cancer (COSMIC, cancer.sanger.ac.uk) (Tate et al. 2019). The functional score of a gene is defined as positive (1, pro-proliferative) if the role of the gene in cancer is an oncogene, and negative (-1, anti-proliferative) if the role of the gene is a tumor suppressor gene (TSG). If a gene has both roles of oncogene and TSG, the functional score is not defined.

Combination perturbation experiments for candidate validation

Experimental validation of the proposed combination candidates was performed by Charles River Laboratories. Six cell lines were used in the experiments, including IGROV-1 (NCI #0507369), OVCAR-4 (NCI #0502527), OVCAR-5 (NCI #0507336), OVCAR-8 (NCI #0507407), OVSAHO, and TOV-21G (ATCC CRL-11730 Lot#58690706). OVSAHO cells were grown in MCDB105/199 medium supplemented with 10% FBS and 1% Penicillin-Streptomycin. TOV-21G cells were grown in RPMI medium supplemented with 15% FBS and 1% Penicillin-Streptomycin. All other four cell lines were grown in RPMI-1640 medium supplemented with 10% FBS and 1% Penicillin-Streptomycin. All the small-molecule drugs are commercially available: Rucaparib (Selleckchem, #S1098), TVB-2640 (Selleckchem, #S9714), Bortezomib

(Selleckchem, #S1013), Apcin (Selleckchem, #S9605), GC7 (Sigma-Aldrich, #259545), AL101/BMS-906024 (MedChemExpress, #HY-15670), Infigratinib (Selleckchem, #S2183), Everolimus (Selleckchem, #S1120), Ivosidenib (Selleckchem, #S8206), Erlotinib (Selleckchem, #S7786), Palbociclib (Selleckchem, #S1116), Bosutinib (Selleckchem, #S1014), Idelalisib (Selleckchem, #S2226), and Auranofin (Selleckchem, #S4307).

Cells were seeded into 96-well plates for checkerboard assays, in which a 3-fold serial dilution of one compound in the combination candidate was performed vertically down the plate for 6 dilution points, and a 3-fold serial dilution of the other compound was performed horizontally across the plate for 9 dilution points. One column of DMSO controls was included for each plate. A 3-fold serial dilution of 6 dilution points was also performed for each compound in single-drug treatment experiments. Different concentration ranges were tested for different compounds for the best outcome: Rucaparib (6 3-fold dilution from 150 μM to 0.62 μM), TVB-2640 (9 3-fold dilution from 180 μM to 0.027 μM), Bortezomib (9 3-fold dilution from 210 nM to 0.032 nM), Apcin and GC7 (9 3-fold dilution from 360 μM to 0.055 μM). Cell viability was measured using CellTiter-Glo assay 72 hr after drug treatment. Synergy scores were calculated using the SynergyFinder R package (Zheng et al. 2022).

Funding

This work received funding from the Ludwig Cancer Center at Harvard Medical School, the National Resource for Network Biology (NRNB) from the National Institute of General Medical Sciences (NIGMS P41 GM103504), and support in part by the Division of Intramural Research (DIR) of the National Library of Medicine (NLM), National Institutes of Health (NIH).

Author Contribution

AF, CiSh, FC, MM, CS were involved in the conceptualization of the study; AF, CiSh, FC, MM worked on collecting the data; AF, CiSh, KM, LC worked to perform investigative experiments; AF, CiSh, AL wrote and ran analysis scripts; AL, CS, MM carried out various supervisory

functions; AF, CiSh, AL, AK, CS analyzed the data. AF, CiSh, AL, CS wrote the original draft along with original figures, all authors reviewed and edited the final manuscript.

Availability of data and materials

Data is provided within the manuscript or supplementary information files.

Declarations

Ethics approval and consent to participate

Not applicable.

Consent for publication

Not applicable.

Competing interests

CS: SAB: Cytoreason Ltd. No disclosures were reported by the other authors.

References

Albrecht, Lauren V., Nydia Tejeda-Muñoz, Maggie H. Bui, Andrew C. Cicchetto, Daniele Di Biagio, Gabriele Colozza, Ernst Schmid, Stefano Piccolo, Heather R. Christofk, and Edward M. De Robertis. 2020. "GSK3 Inhibits Macropinocytosis and Lysosomal Activity through the Wnt Destruction Complex Machinery." *Cell Reports* 32 (4): 107973.

Al-Lazikani, Bissan, Udai Banerji, and Paul Workman. 2012. "Combinatorial Drug Therapy for Cancer in the Post-Genomic Era." *Nature Biotechnology* 30 (7): 679–92.

Arif, Waqar, Gandhar Datar, and Auinash Kalsotra. 2017. "Intersections of Post-Transcriptional Gene Regulatory Mechanisms with Intermediary Metabolism." *Biochimica et Biophysica Acta. Gene Regulatory Mechanisms* 1860 (3): 349–62.

Bajor, Malgorzata, Agnieszka Graczyk-Jarzynka, Katsiaryna Marhelava, Malgorzata Kurkowiak, Arman

Rahman, Claudia Aura, Niamh Russell, et al. 2020. “Triple Combination of Ascorbate, Menadione and the Inhibition of Peroxiredoxin-1 Produces Synergistic Cytotoxic Effects in Triple-Negative Breast Cancer Cells.” *Antioxidants & Redox Signaling* 9 (4): 320.

Baselga, José, Javier Cortés, Sung-Bae Kim, Seock-Ah Im, Roberto Hegg, Young-Hyuck Im, Laslo Roman, et al. 2012. “Pertuzumab plus Trastuzumab plus Docetaxel for Metastatic Breast Cancer.” *The New England Journal of Medicine* 366 (2): 109–19.

Beadnell, Thomas C., Kelsey W. Nassar, Madison M. Rose, Erin G. Clark, Brian P. Danysh, Marie-Claude Hofmann, Nikita Pozdeyev, and Rebecca E. Schweppe. 2018. “Src-Mediated Regulation of the PI3K Pathway in Advanced Papillary and Anaplastic Thyroid Cancer.” *Oncogenesis* 7 (2): 1–14.

Bell, Charles C., Katie A. Fennell, Yih-Chih Chan, Florian Rambow, Miriam M. Yeung, Dane Vassiliadis, Luis Lara, et al. 2019. “Targeting Enhancer Switching Overcomes Non-Genetic Drug Resistance in Acute Myeloid Leukaemia.” *Nature Communications* 10 (1): 2723.

Berns, Els M. J. J., and David D. Bowtell. 2012. “The Changing View of High-Grade Serous Ovarian Cancer.” *Cancer Research* 72 (11): 2701–4.

Bowtell, David D., Steffen Böhm, Ahmed A. Ahmed, Paul-Joseph Aspuria, Robert C. Bast Jr, Valerie Beral, Jonathan S. Berek, et al. 2015. “Rethinking Ovarian Cancer II: Reducing Mortality from High-Grade Serous Ovarian Cancer.” *Nature Reviews. Cancer* 15 (11): 668–79.

Cancer Genome Atlas Research Network. 2011. “Integrated Genomic Analyses of Ovarian Carcinoma.” *Nature* 474 (7353): 609–15.

Carracedo, Arkaitz, Li Ma, Julie Teruya-Feldstein, Federico Rojo, Leonardo Salmena, Andrea Alimonti, Ainara Egia, et al. 2008. “Inhibition of mTORC1 Leads to MAPK Pathway Activation through a PI3K-Dependent Feedback Loop in Human Cancer.” *The Journal of Clinical Investigation* 118 (9): 3065–74.

Cerami, Ethan, Emek Demir, Nikolaus Schultz, Barry S. Taylor, and Chris Sander. 2010. “Automated Network Analysis Identifies Core Pathways in Glioblastoma.” *PloS One* 5 (2): e8918.

Chaudhry, Saliha, Stefani N. Thomas, and Glenn E. Simmons Jr. 2022. “Targeting Lipid Metabolism in the Treatment of Ovarian Cancer.” *Oncotarget* 13 (May):768–83.

Chen, Rain R., Mingo M. H. Yung, Yang Xuan, Shijie Zhan, Leanne L. Leung, Rachel R. Liang, Thomas H. Y. Leung, et al. 2019. “Targeting of Lipid Metabolism with a Metabolic Inhibitor Cocktail Eradicates Peritoneal Metastases in Ovarian Cancer Cells.” *Communications Biology* 2 (July):281.

Chou, Ting-Chao. 2010. “Drug Combination Studies and Their Synergy Quantification Using the Chou-Talalay Method.” *Cancer Research* 70 (2): 440–46.

Colombo, Nicoletta, Domenica Lorusso, and Paolo Scollo. 2017. “Impact of Recurrence of Ovarian Cancer on Quality of Life and Outlook for the Future.” *International Journal of Gynecologic Cancer*. https://doi.org/10.1097/igc.0000000000001023.

Coscia, F., K. M. Watters, M. Curtis, M. A. Eckert, C. Y. Chiang, S. Tyanova, A. Montag, R. R. Lastra, E. Lengyel, and M. Mann. 2016. “Integrative Proteomic Profiling of Ovarian Cancer Cell Lines Reveals Precursor Cell Associated Proteins and Functional Status.” *Nature Communications* 7 (August):12645.

Dahl, Erika S., Raquel Buj, Kelly E. Leon, Jordan M. Newell, Yuka Imamura, Benjamin G. Bitler, Nathaniel W. Snyder, and Katherine M. Aird. 2019. “Targeting IDH1 as a Prosenescent Therapy in High-Grade Serous Ovarian Cancer.” *Molecular Cancer Research: MCR* 17 (8): 1710–20.

Dall’Acqua, Alessandra, Michele Bartoletti, Nastaran Masoudi-Khoram, Roberto Sorio, Fabio Puglisi, Barbara Belletti, and Gustavo Baldassarre. 2021. “Inhibition of CDK4/6 as Therapeutic Approach for Ovarian Cancer Patients: Current Evidences and Future Perspectives.” *Cancers* 13 (12). https://doi.org/10.3390/cancers13123035.

Davidson, Shawn M., and Matthew G. Vander Heiden. 2017. “Critical Functions of the Lysosome in Cancer Biology.” *Annual Review of Pharmacology and Toxicology*. https://doi.org/10.1146/annurev-pharmtox-010715-103101.

Dibra, Denada, Shunbin Xiong, Sydney M. Moyer, Adel K. El-Naggar, Yuan Qi, Xiaoping Su, Elisabeth K. Kong, Anil Korkut, and Guillermina Lozano. 2024. “Mutant p53 Protects Triple-Negative Breast

828 Adenocarcinomas from Ferroptosis in Vivo." *Science Advances* 10 (7): eadk1835.
829 Dodson, Matthew, Raul Castro-Portuguez, and Donna D. Zhang. 2019. "NRF2 Plays a Critical Role in
830 Mitigating Lipid Peroxidation and Ferroptosis." *Redox Biology* 23 (May):101107.
831 Domcke, Silvia, Rileen Sinha, Douglas A. Levine, Chris Sander, and Nikolaus Schultz. 2013. "Evaluating
832 Cell Lines as Tumour Models by Comparison of Genomic Profiles." *Nature Communications*
833 4:2126.
834 Dréan, Amy, Christopher J. Lord, and Alan Ashworth. 2016. "PARP Inhibitor Combination Therapy."
835 *Critical Reviews in Oncology/hematology* 108 (December):73–85.
836 Eaton, John K., Laura Furst, Richard A. Ruberto, Dieter Moosmayer, André Hilpmann, Matthew J. Ryan,
837 Katja Zimmermann, et al. 2020. "Selective Covalent Targeting of GPX4 Using Masked Nitrile-
838 Oxide Electrophiles." *Nature Chemical Biology* 16 (5): 497–506.
839 Fang, Yong, Daniel J. McGrail, Chaoyang Sun, Marilyne Labrie, Xiaohua Chen, Dong Zhang, Zhenlin
840 Ju, et al. 2019. "Sequential Therapy with PARP and WEE1 Inhibitors Minimizes Toxicity While
841 Maintaining Efficacy." *Cancer Cell* 35 (6): 851–67.e7.
842 Feng, Qi, Sheng Hao, Peng Fang, Peng Zhang, and Xiugui Sheng. 2023. "Role of GPX4 Inhibition-
843 Mediated Ferroptosis in the Chemoresistance of Ovarian Cancer to Taxol in Vitro." *Molecular*
844 *Biology Reports* 50 (12): 10189–98.
845 Franciosa, Giulia, Marie Locard-Paulet, Lars J. Jensen, and Jesper V. Olsen. 2023. "Recent Advances in
846 Kinase Signaling Network Profiling by Mass Spectrometry." *Current Opinion in Chemical Biology*
847 73 (April):102260.
848 Franz, Alexandra, Fabian Coscia, Ciyue Shen, Lea Charaoui, Matthias Mann, and Chris Sander. 2021.
849 "Molecular Response to PARP1 Inhibition in Ovarian Cancer Cells as Determined by Mass
850 Spectrometry Based Proteomics." *Journal of Ovarian Research* 14 (1): 1–14.
851 Gao, Min, Jian Deng, Fang Liu, Aiping Fan, Yujuan Wang, Huiyuan Wu, Dan Ding, et al. 2019.
852 "Triggered Ferroptotic Polymer Micelles for Reversing Multidrug Resistance to Chemotherapy."
853 *Biomaterials* 223 (December):119486.
854 Gaschler, Michael M., Alexander A. Andia, Hengrui Liu, Joleen M. Csuka, Brisa Hurlocker, Christopher
855 A. Vaiana, Daniel W. Heindel, et al. 2018. "FINO Initiates Ferroptosis through GPX4 Inactivation
856 and Iron Oxidation." *Nature Chemical Biology* 14 (5): 507–15.
857 Gillespie, Marc, Bijay Jassal, Ralf Stephan, Marija Milacic, Karen Rothfels, Andrea Senff-Ribeiro,
858 Johannes Griss, et al. 2022. "The Reactome Pathway Knowledgebase 2022." *Nucleic Acids Research*
859 50 (D1): D687–92.
860 Gonçalves, Emanuel, Rebecca C. Poulos, Zhaoxiang Cai, Syd Barthorpe, Srikanth S. Manda, Natasha
861 Lucas, Alexandra Beck, et al. 2022. "Pan-Cancer Proteomic Map of 949 Human Cell Lines." *Cancer*
862 *Cell* 40 (8): 835–49.e8.
863 González-Martín, Antonio, Bhavana Pothuri, Ignace Vergote, René DePont Christensen, Whitney
864 Graybill, Mansoor R. Mirza, Colleen McCormick, et al. 2019. "Niraparib in Patients with Newly
865 Diagnosed Advanced Ovarian Cancer." *The New England Journal of Medicine* 381 (25): 2391–
866 2402.
867 Gyori, Benjamin M., John A. Bachman, Kartik Subramanian, Jeremy L. Muhlich, Lucian Galescu, and
868 Peter K. Sorger. 2017. "From Word Models to Executable Models of Signaling Networks Using
869 Automated Assembly." *Molecular Systems Biology* 13 (11): 954.
870 Hangauer, Matthew J., Vasanthi S. Viswanathan, Matthew J. Ryan, Dhruv Bole, John K. Eaton,
871 Alexandre Matov, Jacqueline Galeas, et al. 2017. "Drug-Tolerant Persister Cancer Cells Are
872 Vulnerable to GPX4 Inhibition." *Nature* 551 (7679): 247–50.
873 Hong, Ting, Guang Lei, Xue Chen, He Li, Xiaoye Zhang, Nayiyuan Wu, Yu Zhao, Yilei Zhang, and Jing
874 Wang. 2021. "PARP Inhibition Promotes Ferroptosis via Repressing SLC7A11 and Synergizes with
875 Ferroptosis Inducers in BRCA-Proficient Ovarian Cancer." *Redox Biology* 42 (June):101928.
876 Ioannou, Nikolaos, Alan M. Seddon, Angus Dalgleish, David Mackintosh, and Helmout Modjtahedi.
877 2013. "Treatment with a Combination of the ErbB (HER) Family Blocker Afatinib and the IGF-IR
878 Inhibitor, NVP-AEW541 Induces Synergistic Growth Inhibition of Human Pancreatic Cancer Cells."

879 *BMC Cancer* 13 (1): 1–12.
880 Iorio, Francesco, Theo A. Knijnenburg, Daniel J. Vis, Graham R. Bignell, Michael P. Menden, Michael
881 Schubert, Nanne Aben, et al. 2016. "A Landscape of Pharmacogenomic Interactions in Cancer." *Cell*
882 166 (3): 740–54.
883 Ji, Zhaodong, Yan Shen, Xu Feng, Yue Kong, Yang Shao, Jiao Meng, Xiaofei Zhang, and Gong Yang.
884 2020. "Deregulation of Lipid Metabolism: The Critical Factors in Ovarian Cancer." *Frontiers in*
885 *Oncology* 10 (October):593017.
886 Kalinina, E. V., T. T. Berezov, A. A. Shtil', N. N. Chernov, V. A. Glazunova, M. D. Novichkova, and N.
887 K. Nurmuradov. 2012. "Expression of Peroxiredoxin 1, 2, 3, and 6 Genes in Cancer Cells during
888 Drug Resistance Formation." *Bulletin of Experimental Biology and Medicine* 153 (6): 878–81.
889 Katoh, Masuko, and Masaru Katoh. 2020. "Precision Medicine for Human Cancers with Notch Signaling
890 Dysregulation (Review)." *International Journal of Molecular Medicine* 45 (2): 279–97.
891 Koleti, Amar, Raymond Terryn, Vasileios Stathias, Caty Chung, Daniel J. Cooper, John P. Turner, Dušica
892 Vidovic, et al. 2018. "Data Portal for the Library of Integrated Network-Based Cellular Signatures
893 (LINCS) Program: Integrated Access to Diverse Large-Scale Cellular Perturbation Response Data."
894 *Nucleic Acids Research* 46 (D1): D558–66.
895 Kondrashova, Olga, Monique Topp, Ksenija Nesic, Elizabeth Lieschke, Gwo-Yaw Ho, Maria I. Harrell,
896 Giada V. Zapparoli, et al. 2018. "Methylation of All BRCA1 Copies Predicts Response to the PARP
897 Inhibitor Rucaparib in Ovarian Carcinoma." *Nature Communications* 9 (1): 3970.
898 Kupcik, Rudolf, Jan M. Macak, Helena Rehulkova, Hanna Sopha, Ivo Fabrik, V. C. Anitha, Jana
899 Klimentova, Pavla Murasova, Zuzana Bilkova, and Pavel Rehulka. 2019. "Amorphous TiO
900 Nanotubes as a Platform for Highly Selective Phosphopeptide Enrichment." *ACS Omega* 4 (7):
901 12156–66.
902 Kurimchak, Alison M., Claude Shelton, Kelly E. Duncan, Katherine J. Johnson, Jennifer Brown, Shane
903 O'Brien, Rashid Gabbasov, et al. 2016. "Resistance to BET Bromodomain Inhibitors Is Mediated by
904 Kinome Reprogramming in Ovarian Cancer." *Cell Reports* 16 (5): 1273–86.
905 Lamb, Justin, Emily D. Crawford, David Peck, Joshua W. Modell, Irene C. Blat, Matthew J. Wrobel, Jim
906 Lerner, et al. 2006. "The Connectivity Map: Using Gene-Expression Signatures to Connect Small
907 Molecules, Genes, and Disease." *Science* 313 (5795): 1929–35.
908 Lee, Cha Len, Mattia Cremona, Angela Farrelly, Julie A. Workman, Sean Kennedy, Razia Aslam, Aoife
909 Carr, et al. 2023. "Preclinical Evaluation of the CDK4/6 Inhibitor Palbociclib in Combination with a
910 PI3K or MEK Inhibitor in Colorectal Cancer." *Cancer Biology & Therapy* 24 (1): 2223388.
911 Lee, Michael J., Albert S. Ye, Alexandra K. Gardino, Anne Margriet Heijink, Peter K. Sorger, Gavin
912 MacBeath, and Michael B. Yaffe. 2012. "Sequential Application of Anticancer Drugs Enhances Cell
913 Death by Rewiring Apoptotic Signaling Networks." *Cell* 149 (4): 780–94.
914 Lee, Ronald F. S., Alexey Chernobrovkin, Dorothea Rutishauser, Claire S. Allardyce, David Hacker, Kai
915 Johnsson, Roman A. Zubarev, and Paul J. Dyson. 2017. "Expression Proteomics Study to Determine
916 Metallodrug Targets and Optimal Drug Combinations." *Scientific Reports* 7 (1): 1–11.
917 Lei, Guang, Chao Mao, Amber D. Horbath, Yuelong Yan, Shirong Cai, Jun Yao, Yan Jiang, et al. 2024.
918 "BRCA1-Mediated Dual Regulation of Ferroptosis Exposes a Vulnerability to GPX4 and PARP Co-
919 Inhibition in BRCA1-Deficient Cancers." *Cancer Discovery* 14 (8): 1476–95.
920 Li, Jiaran, Jifeng Wang, Yumeng Yan, Na Li, Xiaoqing Qing, Ailikemu Tuerxun, Xiaojing Guo, Xiulan
921 Chen, and Fuquan Yang. 2022. "Comprehensive Evaluation of Different TiO-Based Phosphopeptide
922 Enrichment and Fractionation Methods for Phosphoproteomics." *Cells* 11 (13).
923 https://doi.org/10.3390/cells11132047.
924 Li, Ning, Xingmei Jiang, Qingyu Zhang, Yongmei Huang, Jinbin Wei, Haitao Zhang, and Hui Luo. 2024.
925 "Synergistic Suppression of Ovarian Cancer by Combining NRF2 and GPX4 Inhibitors: In Vitro and
926 in Vivo Evidence." *Journal of Ovarian Research* 17 (1): 49.
927 Liu, Eric Minwei, Augustin Luna, Guanlan Dong, and Chris Sander. 2020. "Netboxr: Automated
928 Discovery of Biological Process Modules by Network Analysis in R." *PloS One* 15 (11): e0234669.
929 Li, Wenhua, Xiaoying Liu, Xu Cheng, Wenyuan Zhang, Chen Gong, Chuya Gao, Haisheng Peng, Bo

930 Yang, Shukun Tang, and Haiquan Tao. 2022. “Effect of Malt-PEG-Abz@RSL3 Micelles on HepG2
931 Cells Based on NADPH Depletion and GPX4 Inhibition in Ferroptosis.” *Journal of Drug Targeting*
932 30 (2): 208–18.
933 Long, Georgina V., Jeffrey S. Weber, Jeffrey R. Infante, Kevin B. Kim, Adil Daud, Rene Gonzalez,
934 Jeffrey A. Sosman, et al. 2016. “Overall Survival and Durable Responses in Patients With BRAF
935 V600-Mutant Metastatic Melanoma Receiving Dabrafenib Combined With Trametinib.” *Journal of*
936 *Clinical Oncology: Official Journal of the American Society of Clinical Oncology* 34 (8): 871–78.
937 Lu, Xue, Yaowu He, Rebecca L. Johnston, Devathri Nanayakarra, Sivanandhini Sankarasubramanian, J.
938 Alejandro Lopez, Michael Friedlander, et al. 2022. “CBL0137 Impairs Homologous Recombination
939 Repair and Sensitizes High-Grade Serous Ovarian Carcinoma to PARP Inhibitors.” *Journal of*
940 *Experimental & Clinical Cancer Research: CR* 41 (1): 355.
941 Marine, Jean-Christophe, Sarah-Jane Dawson, and Mark A. Dawson. 2020. “Non-Genetic Mechanisms of
942 Therapeutic Resistance in Cancer.” *Nature Reviews. Cancer* 20 (12): 743–56.
943 Matulonis, Ursula A., Anil K. Sood, Lesley Fallowfield, Brooke E. Howitt, Jalid Sehouli, and Beth Y.
944 Karlan. 2016. “Ovarian Cancer.” *Nature Reviews Disease Primers* 2 (1): 1–22.
945 Matusewicz, Lucyna, Justyna Meissner, Monika Toporkiewicz, and Aleksander F. Sikorski. 2015. “The
946 Effect of Statins on Cancer Cells--Review.” *Tumour Biology: The Journal of the International*
947 *Society for Oncodevelopmental Biology and Medicine* 36 (7): 4889–4904.
948 Mayer, Erica L., and Ian E. Krop. 2010. “Advances in Targeting SRC in the Treatment of Breast Cancer
949 and Other Solid Malignancies.” *Clinical Cancer Research: An Official Journal of the American*
950 *Association for Cancer Research* 16 (14): 3526–32.
951 Munir, Rimsha, Jan Lisec, Johannes V. Swinnen, and Nousheen Zaidi. 2019. “Lipid Metabolism in
952 Cancer Cells under Metabolic Stress.” *British Journal of Cancer* 120 (12): 1090–98.
953 Nayman, Ayse Hande, Halime Siginc, Ebru Zemheri, Faruk Yencilek, Asif Yildirim, and Dilek Telci.
954 2019. “Dual-Inhibition of mTOR and Bcl-2 Enhances the Anti-Tumor Effect of Everolimus against
955 Renal Cell Carcinoma and.” *Journal of Cancer* 10 (6): 1466–78.
956 Nguyen, Mai Q., Jessica L. F. Teh, Timothy J. Purwin, Inna Chervoneva, Michael A. Davies, Katherine
957 L. Nathanson, Phil F. Cheng, Mitchell P. Levesque, Reinhard Dummer, and Andrew E. Aplin. 2020.
958 “Targeting PHGDH Upregulation Reduces Glutathione Levels and Resensitizes Resistant NRAS-
959 Mutant Melanoma to MAPK Kinase Inhibition.” *The Journal of Investigative Dermatology* 140 (11):
960 2242–52.e7.
961 Nicolussi, Arianna, Sonia D’inzeo, Carlo Capalbo, Giuseppe Giannini, and Anna Coppa. 2017. “The Role
962 of Peroxiredoxins in Cancer (Review).” *Molecular and Clinical Oncology* 6 (2): 139–53.
963 Niepel, Mario, Marc Hafner, Qiaonan Duan, Zichen Wang, Evan O. Paull, Mirra Chung, Xiaodong Lu, et
964 al. 2017. “Common and Cell-Type Specific Responses to Anti-Cancer Drugs Revealed by High
965 Throughput Transcript Profiling.” *Nature Communications* 8 (1): 1–11.
966 Olsauskas-Kuprys, Roma, Andrei Zlobin, and Clodia Osipo. 2013. “Gamma Secretase Inhibitors of Notch
967 Signaling.” *OncoTargets and Therapy* 6 (July):943–55.
968 O’Reilly, Kathryn E., Fredi Rojo, Qing-Bai She, David Solit, Gordon B. Mills, Debra Smith, Heidi Lane,
969 et al. 2006. “mTOR Inhibition Induces Upstream Receptor Tyrosine Kinase Signaling and Activates
970 Akt.” *Cancer Research* 66 (3): 1500–1508.
971 Packer, Leisl M., Samantha J. Stehbens, Vanessa F. Bonazzi, Jennifer H. Gunter, Robert J. Ju, Micheal
972 Ward, Michael G. Gartside, Sara A. Byron, and Pamela M. Pollock. 2019. “Bcl-2 Inhibitors Enhance
973 FGFR Inhibitor-Induced Mitochondrial-Dependent Cell Death in FGFR2-Mutant Endometrial
974 Cancer.” *Molecular Oncology* 13 (4): 738–56.
975 Palmer, Adam C., and Peter K. Sorger. 2017. “Combination Cancer Therapy Can Confer Benefit via
976 Patient-to-Patient Variability without Drug Additivity or Synergy.” *Cell* 171 (7): 1678–91.e13.
977 Peng, Xin, Xin Huang, Shaolu Zhang, Naixin Zhang, Shengfan Huang, Yingying Wang, Zhenxing
978 Zhong, et al. 2024. “Sequential Inhibition of PARP and BET as a Rational Therapeutic Strategy for
979 Glioblastoma.” *Advancement of Science* 11 (30): e2307747.
980 Perkins, Arden, Kimberly J. Nelson, Derek Parsonage, Leslie B. Poole, and P. Andrew Karplus. 2015.

"Peroxiredoxins: Guardians against Oxidative Stress and Modulators of Peroxide Signaling." *Trends in Biochemical Sciences* 40 (8): 435–45.

Rexer, Brent N., and Carlos L. Arteaga. 2012. "Intrinsic and Acquired Resistance to HER2-Targeted Therapies in HER2 Gene-Amplified Breast Cancer: Mechanisms and Clinical Implications." *Critical Reviews in Oncogenesis* 17 (1): 1–16.

Robert, Caroline, Georgina V. Long, Benjamin Brady, Caroline Dutriaux, Michele Maio, Laurent Mortier, Jessica C. Hassel, et al. 2015. "Nivolumab in Previously Untreated Melanoma without BRAF Mutation." *The New England Journal of Medicine* 372 (4): 320–30.

Roelants, Caroline, Sofia Giacosa, Catherine Pillet, Rémi Bussat, Pierre Champelovier, Olivier Bastien, Laurent Guyon, Valentin Arnoux, Claude Cochet, and Odile Filhol. 2018. "Combined Inhibition of PI3K and Src Kinases Demonstrates Synergistic Therapeutic Efficacy in Clear-Cell Renal Carcinoma." *Oncotarget* 9 (53): 30066–78.

Ruocco, Maria Rosaria, Angelica Avagliano, Giuseppina Granato, Elena Vigliar, Stefania Masone, Stefania Montagnani, and Alessandro Arcucci. 2019. "Metabolic Flexibility in Melanoma: A Potential Therapeutic Target." *Seminars in Cancer Biology* 59 (December):187–207.

Ruprecht, Benjamin, Julie Di Bernardo, Zhao Wang, Xuan Mo, Oleg Ursu, Matthew Christopher, Rafael B. Fernandez, et al. 2020. "A Mass Spectrometry-Based Proteome Map of Drug Action in Lung Cancer Cell Lines." *Nature Chemical Biology* 16 (10): 1111–19.

Saei, Amir Ata, Christian Michel Beusch, Alexey Chernobrovkin, Pierre Sabatier, Bo Zhang, Ülkü Güler Tokat, Eleni Stergiou, Massimiliano Gaetani, Ákos Végvári, and Roman A. Zubarev. 2019. "ProTargetMiner as a Proteome Signature Library of Anticancer Molecules for Functional Discovery." *Nature Communications* 10 (1): 1–13.

Settleman, Jeff, João M. Fernandes Neto, and René Bernards. 2021. "Thinking Differently about Cancer Treatment Regimens." *Cancer Discovery* 11 (5): 1016–23.

Shin, Daiha, Eun Hye Kim, Jaewang Lee, and Jong-Lyel Roh. 2018. "Nrf2 Inhibition Reverses Resistance to GPX4 Inhibitor-Induced Ferroptosis in Head and Neck Cancer." *Free Radical Biology & Medicine* 129 (December):454–62.

Siddiqui, Arafat, Manuela Tumiati, Alia Joko, Jouko Sandholm, Pia Roering, Sofia Aakko, Reetta Vainionpää, et al. 2021. "Targeting DNA Homologous Repair Proficiency With Concomitant Topoisomerase II and c-Abl Inhibition." *Frontiers in Oncology* 11 (September):733700.

Siegel, Rebecca L., Kimberly D. Miller, and Ahmedin Jemal. 2019. "Cancer Statistics, 2019." *CA: A Cancer Journal for Clinicians* 69 (1): 7–34.

Sinha, Rileen, Augustin Luna, Nikolaus Schultz, and Chris Sander. 2021. "A Pan-Cancer Survey of Cell Line Tumor Similarity by Feature-Weighted Molecular Profiles." *Cell Reports Methods* 1 (2): 100039.

Snaebjornsson, Marteinn Thor, Sudha Janaki-Raman, and Almut Schulze. 2020. "Greasing the Wheels of the Cancer Machine: The Role of Lipid Metabolism in Cancer." *Cell Metabolism* 31 (1): 62–76.

Subramanian, Aravind, Pablo Tamayo, Vamsi K. Mootha, Sayan Mukherjee, Benjamin L. Ebert, Michael A. Gillette, Amanda Paulovich, et al. 2005. "Gene Set Enrichment Analysis: A Knowledge-Based Approach for Interpreting Genome-Wide Expression Profiles." *Proceedings of the National Academy of Sciences of the United States of America* 102 (43): 15545–50.

Tate, John G., Sally Bamford, Harry C. Jubb, Zbyslaw Sondka, David M. Beare, Nidhi Bindal, Harry Boutselakis, et al. 2019. "COSMIC: The Catalogue Of Somatic Mutations In Cancer." *Nucleic Acids Research* 47 (D1): D941–47.

Wang, Liyuan, Xiaoguang Chen, and Chunhong Yan. 2022. "Ferroptosis: An Emerging Therapeutic Opportunity for Cancer." *Genes & Diseases* 9 (2): 334–46.

Wang, Xin-Yan, Hai-Jiao Wang, and Xiu-Qin Li. 2013. "Peroxiredoxin III Protein Expression Is Associated with Platinum Resistance in Epithelial Ovarian Cancer." *Tumour Biology: The Journal of the International Society for Oncodevelopmental Biology and Medicine* 34 (4): 2275–81.

Wilson, Andrew J., Matthew Stubbs, Phillip Liu, Bruce Ruggeri, and Dineo Khabele. 2018. "The BET Inhibitor INCB054329 Reduces Homologous Recombination Efficiency and Augments PARP

Inhibitor Activity in Ovarian Cancer." *Gynecologic Oncology* 149 (3): 575–84.

Wu, Qi, Hanpu Zhang, Si Sun, Lijun Wang, and Shengrong Sun. 2021. "Extracellular Vesicles and Immunogenic Stress in Cancer." *Cell Death & Disease* 12 (10): 894.

Wu, Xiaodong, Shizhen Shen, Jiale Qin, Weidong Fei, Fengyun Fan, Jiaxin Gu, Tao Shen, Tao Zhang, and Xiaodong Cheng. 2022. "High Co-Expression of SLC7A11 and GPX4 as a Predictor of Platinum Resistance and Poor Prognosis in Patients with Epithelial Ovarian Cancer." *BJOG: An International Journal of Obstetrics and Gynaecology* 129 Suppl 2 (Suppl 2): 40–49.

Yan, Gonghong, Augustin Luna, Heping Wang, Behnaz Bozorgui, Xubin Li, Maga Sanchez, Zeynep Dereli, et al. 2022. "BET Inhibition Induces Vulnerability to MCL1 Targeting through Upregulation of Fatty Acid Synthesis Pathway in Breast Cancer." *Cell Reports* 40 (11): 111304.

Yang, Wan Seok, Rohitha SriRamaratnam, Matthew E. Welsch, Kenichi Shimada, Rachid Skouta, Vasanthi S. Viswanathan, Jaime H. Cheah, et al. 2014. "Regulation of Ferroptotic Cancer Cell Death by GPX4." *Cell* 156 (1-2): 317–31.

Yoon, Hyunho, and Sanghoon Lee. 2022. "Fatty Acid Metabolism in Ovarian Cancer: Therapeutic Implications." *International Journal of Molecular Sciences* 23 (4). https://doi.org/10.3390/ijms23042170.

Yuan, Bo, Ciyue Shen, Augustin Luna, Anil Korkut, Debora S. Marks, John Ingraham, and Chris Sander. 2021. "CellBox: Interpretable Machine Learning for Perturbation Biology with Application to the Design of Cancer Combination Therapy." *Cell Systems* 12 (2): 128–40.e4.

Yu, Guangchuang, Li-Gen Wang, Yanyan Han, and Qing-Yu He. 2012. "clusterProfiler: An R Package for Comparing Biological Themes among Gene Clusters." *Omics: A Journal of Integrative Biology* 16 (5): 284–87.

Zaky, Mohamed Y., Chuanwen Fan, Huan Zhang, and Xiao-Feng Sun. 2023. "Unraveling the Anticancer Potential of Statins: Mechanisms and Clinical Significance." *Cancers* 15 (19). https://doi.org/10.3390/cancers15194787.

Zhao, Wei, Jun Li, Mei-Ju M. Chen, Yikai Luo, Zhenlin Ju, Nicole K. Nesser, Katie Johnson-Camacho, et al. 2020. "Large-Scale Characterization of Drug Responses of Clinically Relevant Proteins in Cancer Cell Lines." *Cancer Cell* 38 (6): 829–43.e4.

Zheng, Shuyu, Wenyu Wang, Jehad Aldahdooh, Alina Malyutina, Tolou Shadbahr, Ziaurrehman Tanoli, Alberto Pessia, and Jing Tang. 2022. "SynergyFinder Plus: Toward Better Interpretation and Annotation of Drug Combination Screening Datasets." *Genomics, Proteomics & Bioinformatics*, January. https://doi.org/10.1016/j.gpb.2022.01.004.

Zhou, Jia, Camille Gelot, Constantia Pantelidou, Adam Li, Hatice Yücel, Rachel E. Davis, Anniina Färkkilä, et al. 2021. "A First-in-Class Polymerase Theta Inhibitor Selectively Targets Homologous-Recombination-Deficient Tumors." *Nature Cancer* 2 (6): 598–610.